

Problem Definition:

The geometry, dimensions, boundary conditions, and symmetry of the cello with f-hole surface were defined as shown in **Figure 1**. Using structural analysis, the normal stresses in X and Y direction, von-Mises stress, and the deflection of the cello in Z-direction would be determined after the loading of the bridge on the top face of the cello was applied. Another structural analysis would be done by using a full cello top face model with a smaller surface thickness. Moreover, the first 6 natural frequencies of the cello would be determined and analyzed by using modal analysis that modeled the full cello top face and using another model analysis that used symmetry and modeled only half of the cello.

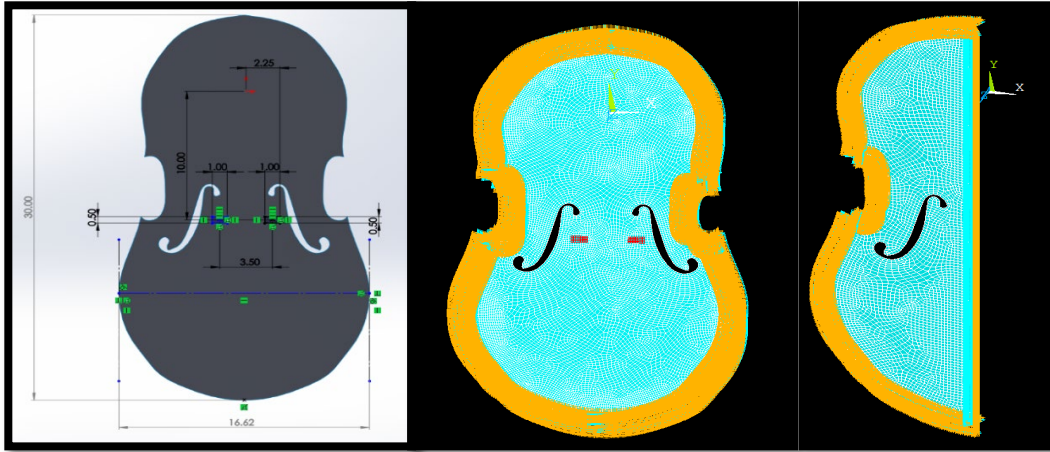


Figure 1: Cello Top Surface with f-hole Geometry, Boundary Conditions and Symmetry.

Description of Analysis Model:

Model Number	Elements Size [in.]	Number of Elements	Thickness [in.]	Orientation [°]	Pressure Load [psi]	Number of Modes to Extract and Expand
1 (Full)	0.20	12884	0.275	90	30	
2 (Full)	0.20	12884	0.275	90		12
3 (Symmetry)	0.20	4418	0.275	90		6
4 (Full)	0.20	12884	0.125	90	30	
5 (Full)	0.20	12884	0.125	90		12

Table 1: A list of Element Type and Behavior Used for the ANSYS Simulation.

Material	Young Modulus			Shear Modulus			Poisson's Ratio		
	E_x , x10 ⁶ psi	E_y , x10 ⁶ psi	E_z , x10 ⁶ psi	G_{xy} , x10 ⁶ psi	G_{yz} , x10 ⁶ psi	G_{xz} , x10 ⁶ psi	ν_{xy}	ν_{yz}	ν_{xz}
Douglas Fir	1.83	0.0915	0.1244	0.143	0.0128	0.117	0.449	0.374	0.292

Table 2: Douglas fir's Structural Linear Elastic Orthotropic Material Properties.

Element type of all the cello models were shell and quadratic quadrilateral; the material of the cello was Douglas fir, and the density of Douglas fir is 0.44×10^{-4} lb.s²/in⁴. A normal pressure of 30 psi was applied on the cello top total surface area of 1.0 in² that were caused by the loading of the bridge. For the boundary condition of the full cello top surface with f-hole, all the outside edges were fixed in all degree of freedoms as shown in **Figure 1**; for the boundary condition of the half cello top surface with f-hole, all the outside edges were fixed in all degree of freedoms except the right vertical edge was fixed in X-displacement ($u_x = 0$ in.), and rotation along y-axis ($\text{rot}_y = 0^\circ$) as shown in **Figure 1**. The units of the analysis model's pressure, force, and length were in psi, lb., and in., respectively.

Summary Results:

Model Number	Thickness [in.]	Maximum Deflection, δ [in.]	Maximum von-Mises Stress, σ' [psi]	Maximum X-normal stress, σ_x [psi]	Maximum Y-normal stress, σ_y [psi]
1 (Full)	0.275	0.076748	2,923.19	1,320.99	3,002.56
4 (Full)	0.125	0.835725	14,600.2	7,638.92	14,952.4

Table 3: Structural Analysis Results

Model Number	Frequency Modes, [Hz]											
	1	2	3	4	5	6	7	8	9	10	11	12
2 (Full)	120.95	171.47	229.17	298.73	320.58	389.63	425.64	440.07	556.15	574.88	601.78	646.03
3 (Symmetry)	111.27	173.62	293.94	424.91	461.22	607.57						
5 (Full)	57.93	82.79	110.12	143.66	154.32	188.45	205.56	211.62	270.46	279.02	291.96	322.14

Table 4: Modal Analysis Results

Based on the **Table 3** structural analysis results, as the thickness of the top cello face with f-hole decreased, the maximum deflection increased by approximately 0.759 in, and the maximum von-Mises Stress of the cello increased by approximately 11,677 psi. According to **Table 4**, the first, second, third, ninth frequency modes of the Modal 2 were symmetry, and the other frequency modes were anti-symmetry; the first six frequency modes of the Model 3 were symmetry. Finally, the first, second, third, ninth frequency modes of the Modal 5 were symmetry, and the other frequency modes were anti-symmetry

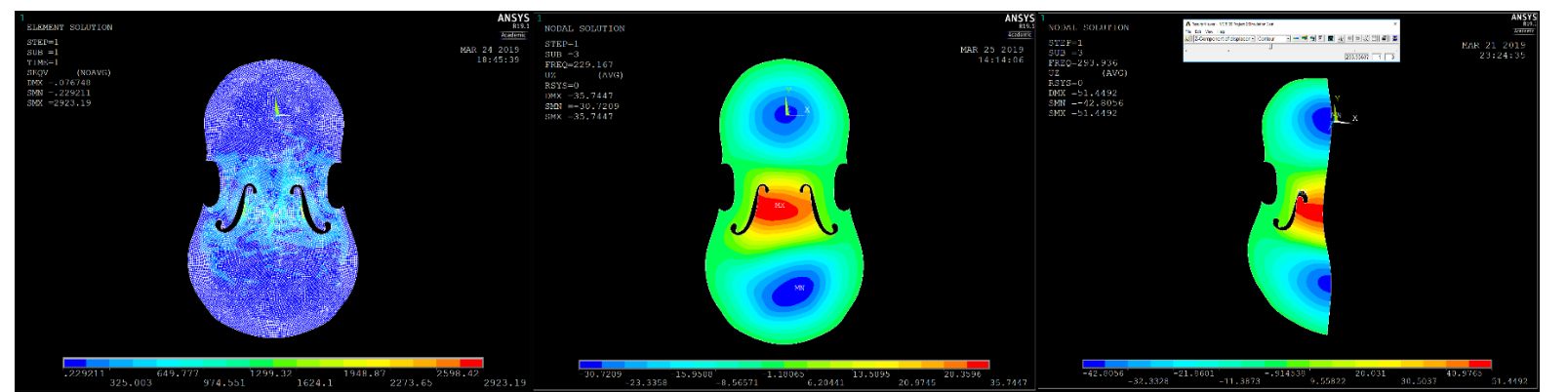


Figure 2: von-Mises Plot for Model 1 (Left), Z-displacement Frequency Mode 3 Plot for Model 2 (Center), and Z-displacement Frequency Mode 3 Plot for Model 3 (Right)

Verifications:

The deflection of the cello in Z-displacement, δ and the maximum normal stress in X-direction, $\sigma_{\max x}$ for Model 1’s structural analysis were verified to be a valid in the ANSYS ADPL simulation (Appendix, Pg 3, 4). The percentage error, %error between the simulation and calculated deflections of the cello in Z-displacement (i.e., $y_{\max \text{ simulation}}$ and $y_{\max 1}$) was determined to be 0.46 %; the simulation maximum normal stress in the x-direction, $\sigma_{\max x \text{ simulation}}$ was determined to fall between both calculated maximum normal stresses in the x-direction (i.e., $\sigma_{\max x1}$ and $\sigma_{\max x2}$) (Appendix, Pg 3, 4). Furthermore, the cello mode 1 natural frequency in the simulation for Model 2’s structural analysis was determined to be valid because the simulated mode 1 natural frequency, $f_{\text{simulation}}$ (i.e., 120.95 Hz) was in between the calculated highest mode 1 natural frequency, f_1 (370 Hz) and the calculated lowest mode 1 natural frequency, f_2 (i.e. 71 Hz) (Appendix, Pg 4, 5).

Conclusion:

Based on the “Becoming a Finite Element Analyst, A Design-Model-Verify Approach” textbook by Dr. Dupaix, the Wood, Douglas fir has an ultimate tensile strength of 7,000 psi. The simulated Maximum Von-Mises Stress for Model 1 with a thickness of 0.275 in was determined to be 2,923.19 psi. Since the simulated Maximum Von-Mises Stress of the cello is smaller than the ultimate tensile strength (i.e., $\sigma_{\text{von-Mises}} < S_{ut}$) and the factor of safety, n , is more than one, the cello will not fail when the pressure load of 30 psi is applied on the cello by the bridge supports (Appendix, Pg 6). On the other hand, the simulated Maximum Von-Mises Stress for Model 4 with a thickness of 0.125 in was determined to be 14,600.2 psi. Since the simulated Maximum Von-Mises Stress of the cello is larger than the ultimate tensile strength (i.e., $\sigma_{\text{von-Mises}} < S_{ut}$) and the factor of safety, n , is less than one, the cello will fail when the pressure load of 30 psi is applied on the cello by the bridge supports (Appendix, Pg 6). When the first twelve natural frequencies were extracted from the full cello top face with f-hole models, which are Model 2 and Model 5, it showed that the thickness of the top face cello affects the natural frequencies in different mode; as the thickness of the top cello surface decreased, the natural frequencies in different modes decreased.

Appendix

Calculations for Verifications:

1. Deflection

$$\frac{b}{a} = \frac{30}{16.62} = 1.8 \quad k_1 = 0.177$$

$$y_{max1} = k_1 \frac{Pa^2}{E_x t^3}$$

$$y_{max1} = 0.177 \frac{60(16.62)^2}{(1.83 \times 10^6)(0.275)^3} = 0.0771 \text{ in.}$$

$$y_{max2} = k_1 \frac{Pa^2}{E_y t^3}$$

$$y_{max2} = 0.177 \frac{60(16.62)^2}{(0.0915 \times 10^6)(0.275)^3} = 1.54 \text{ in.}$$

$$y_{\max \text{ simulation}} = 0.076748 \text{ in.}$$

$$\% \text{ error} = \frac{|y_{\max 1} - y_{\max \text{ simulation}}|}{y_{\max 1}} \times 100\%$$

$$\% \text{ error} = \frac{|0.0771 - 0.076748|}{0.0771} \times 100\%$$

$$\% \text{ error} = 0.46 \%$$

2. Stress

$$k_2 = 0.072$$

$$A_{total} = \pi e^2$$

$$2(1 \times 0.5) = \pi e^2$$

$$e = \sqrt{\frac{1}{\pi}} = 0.5642 \text{ in.}$$

$$\sigma_{max1} = \frac{1.5P}{\pi t^2} \left[(1 + \nu_{xy}) \ln \left(\frac{2a}{\pi e} \right) + 1 - k_2 \right]$$

$$\sigma_{max1} = \frac{1.5(60)}{\pi(0.275)^2} \left[(1 + 0.449) \ln \left(\frac{2(16.62)}{\pi(0.5642)} \right) + 1 - 0.072 \right]$$

$$\sigma_{max1} = 1,167.12 \text{ psi}$$

$$\sigma_{max2} = \frac{1.5P}{\pi t^2} \left[(1 + \nu_{xz}) \ln \left(\frac{2a}{\pi e} \right) + 1 - k_2 \right]$$

$$\sigma_{max2} = \frac{1.5(60)}{\pi(0.275)^2} \left[(1 + 0.292) \ln \left(\frac{2(16.62)}{\pi(0.5642)} \right) + 1 - 0.072 \right]$$

$$\sigma_{max2} = 1,786.24 \text{ psi}$$

$$\sigma_{max \text{ simulation}} = 1,320.99 \text{ psi}$$

$$\sigma_{max1} \leq \sigma_{max \text{ simulation}} \leq \sigma_{max2}$$

3. Frequency

Edge Conditions: C-C-C-C

Mode 1

b = 16.62 in.

a = 30 in.

$$\frac{a}{b} = \frac{30}{16.62} = 1.805$$

Apply interpolation:

$$k - 23.65 = \frac{147.80 - 23.65}{2.5 - 0.4} \times (1.805 - 0.4)$$

$$k = 106.71$$

$$106.71 = \omega_1 a^2 \sqrt{\frac{\rho h}{D}}$$

$$106.71 = \omega_1 (30)^2 \sqrt{\frac{\rho}{\frac{E_x h^2}{12(1 - \nu^2)}}}$$

$$106.71 = \omega_1 (30 \text{ in})^2 \sqrt{\frac{(0.44 \times 10^{-4} \text{ lb} \cdot \frac{\text{s}^2}{\text{in}^4})}{\frac{(1.83 \times 10^6 \text{ lb/in}^2)(0.275 \text{ in})^2}{12(1 - 0.3^2)}}}$$

$$\omega_1 = 2012.26 \frac{\text{rad}}{\text{s}}$$

$$f_1 = \frac{\omega_1}{2\pi} = \frac{2012.26}{2\pi}$$

$$f_1 = 320 \text{ Hz}$$

$$106.71 = \omega_2 a^2 \sqrt{\frac{\rho h}{D}}$$

$$106.71 = \omega_2 (30)^2 \sqrt{\frac{\frac{\rho}{E_y h^2}}{12(1 - \nu^2)}}$$

$$106.71 = \omega_2 (30 \text{ in})^2 \sqrt{\frac{(0.44 \times 10^{-4} \text{ lb} \cdot \frac{\text{s}^2}{\text{in}^4})}{\frac{(0.0915 \times 10^6 \text{ lb/in}^2)(0.275 \text{ in})^2}{12(1 - 0.3^2)}}}$$

$$\omega_2 = 449.95 \frac{\text{rad}}{\text{s}}$$

$$f_2 = \frac{\omega_2}{2\pi} = \frac{449.95}{2\pi}$$

$$f_2 = 71 \text{ Hz}$$

$$f_2 \leq f_{\text{simulation}} \leq f_1$$

4. Safety Factor

Thickness = 0.275 in.

$$\text{Factor of Safety}, n = \frac{S_{\text{ultimate tensile}}}{\sigma_{\text{Maximum Von-Mises}}} = \frac{7000 \text{ psi}}{2923.19 \text{ psi}}$$

$$n = 2.394$$

$$\therefore, n > 1$$

Thickness = 0.125 in.

$$\text{Factor of Safety}, n = \frac{S_{\text{ultimate tensile}}}{\sigma_{\text{Maximum Von-Mises}}} = \frac{7000 \text{ psi}}{14600.2 \text{ psi}}$$

$$n = 0.479$$

$$\therefore, n < 1$$

Results Screenshots:

1. Boundary Conditions

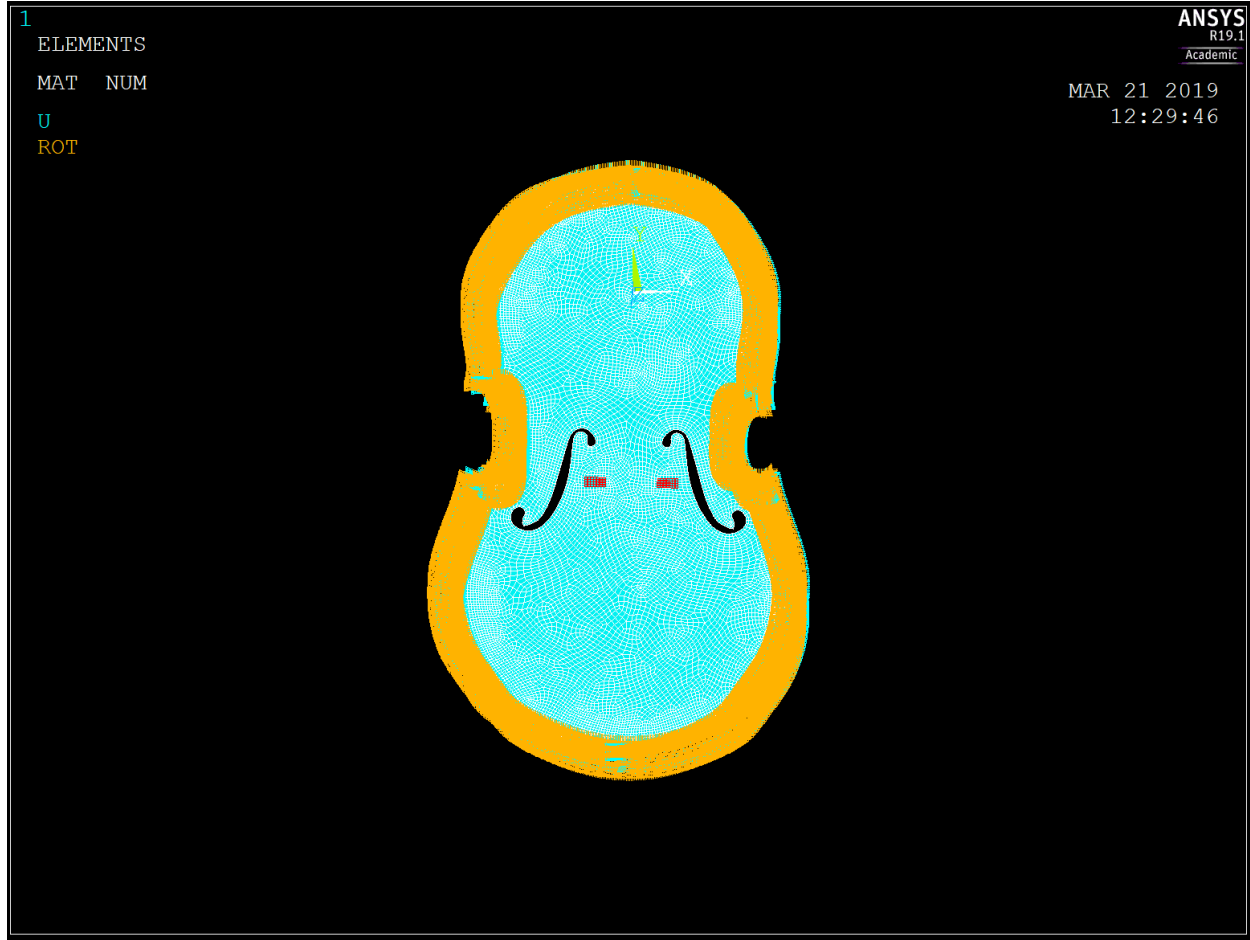


Figure 3: Full Cello Boundary Conditions (Pressure Applied = 30 psi; thickness = 0.275 in; Material: Douglas fir)

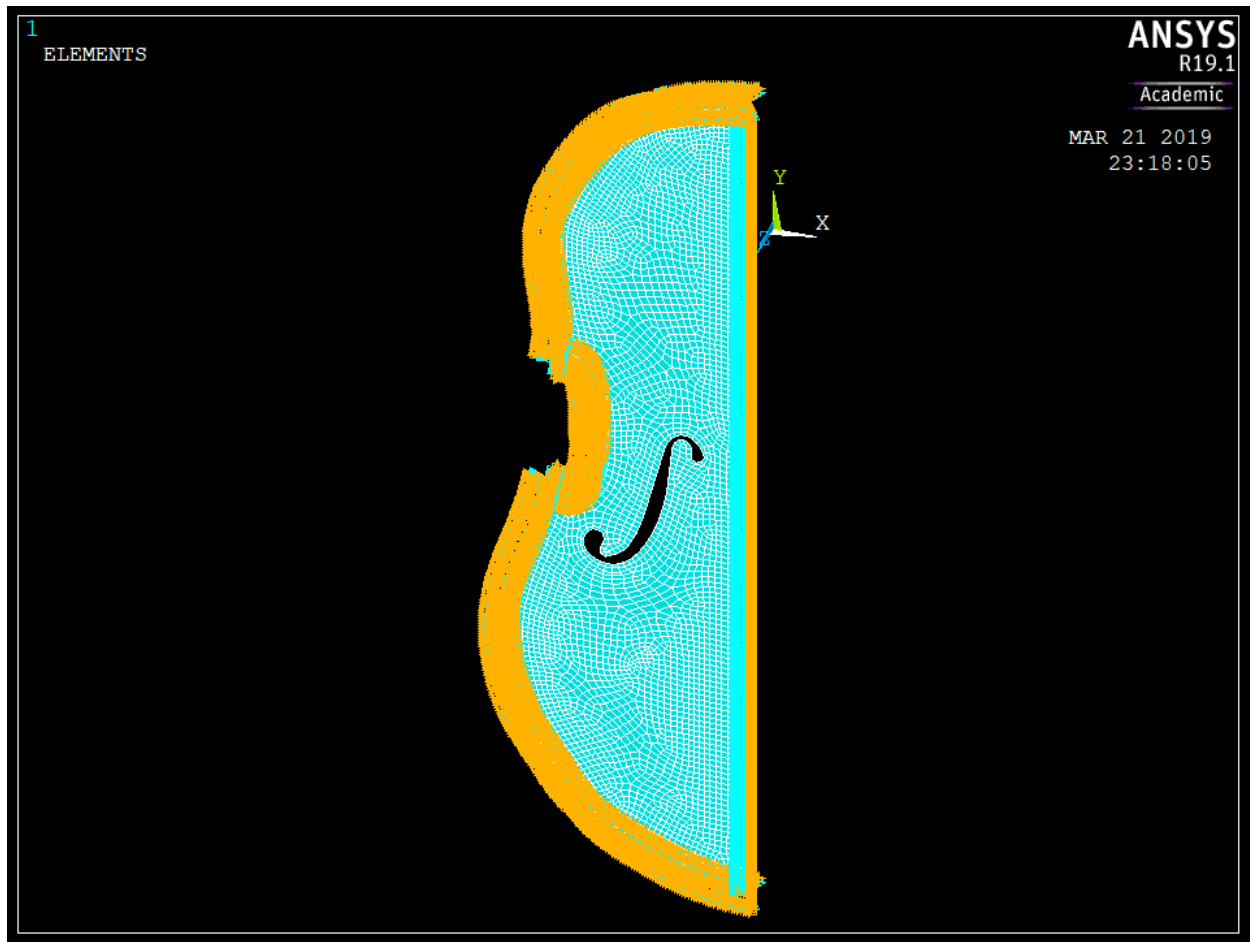


Figure 4: Symmetry Cello Boundary Conditions (Thickness = 0.275 in; Material: Douglas fir) Right Edges was fixed with $u_x=0$ and $roty=0$.

2. Structural Analysis for the First Model



Figure 5: 1st Model Z-Displacement Contour Plot

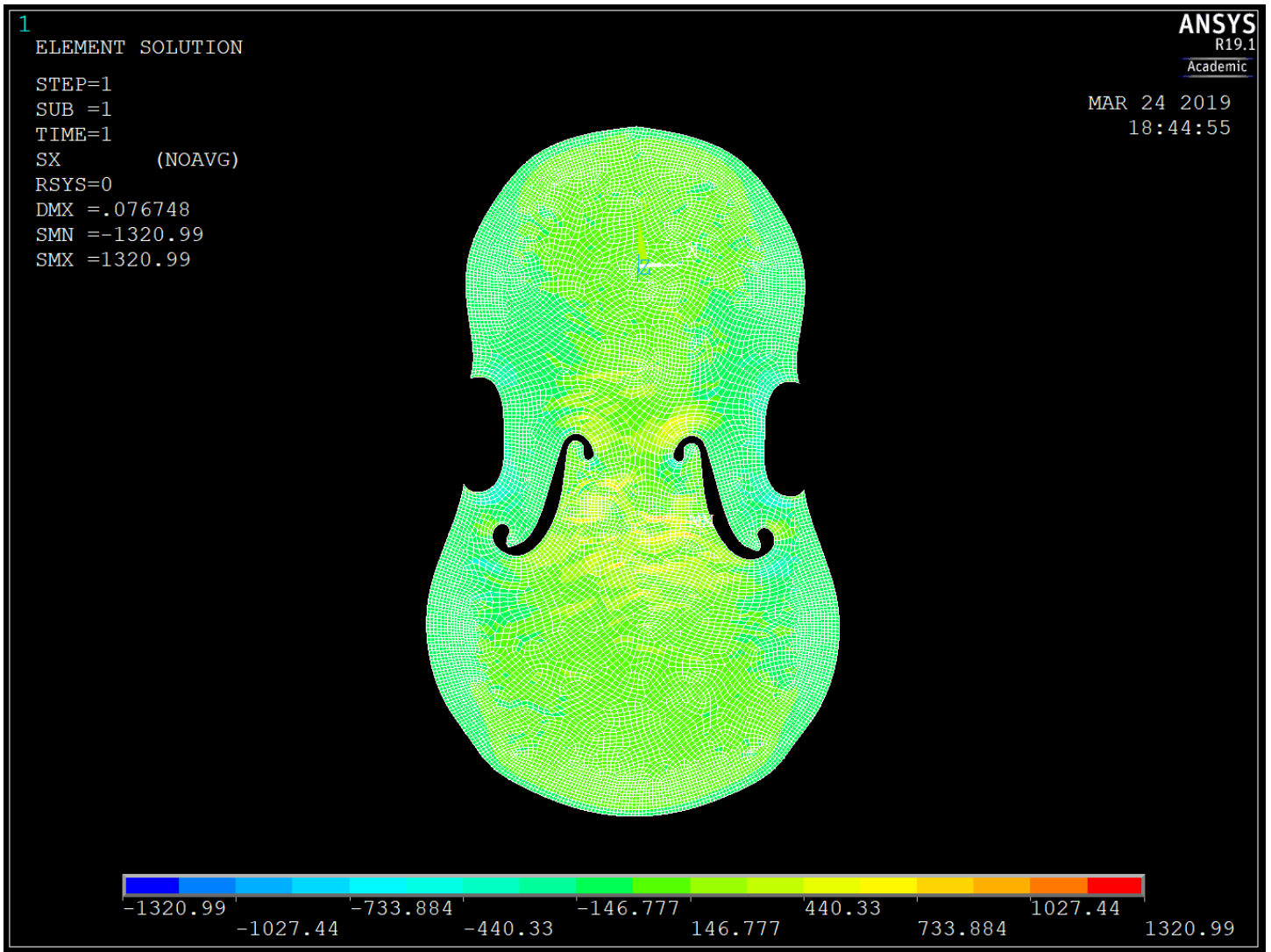


Figure 6: 1st Model X-normal Stress Contour Plot

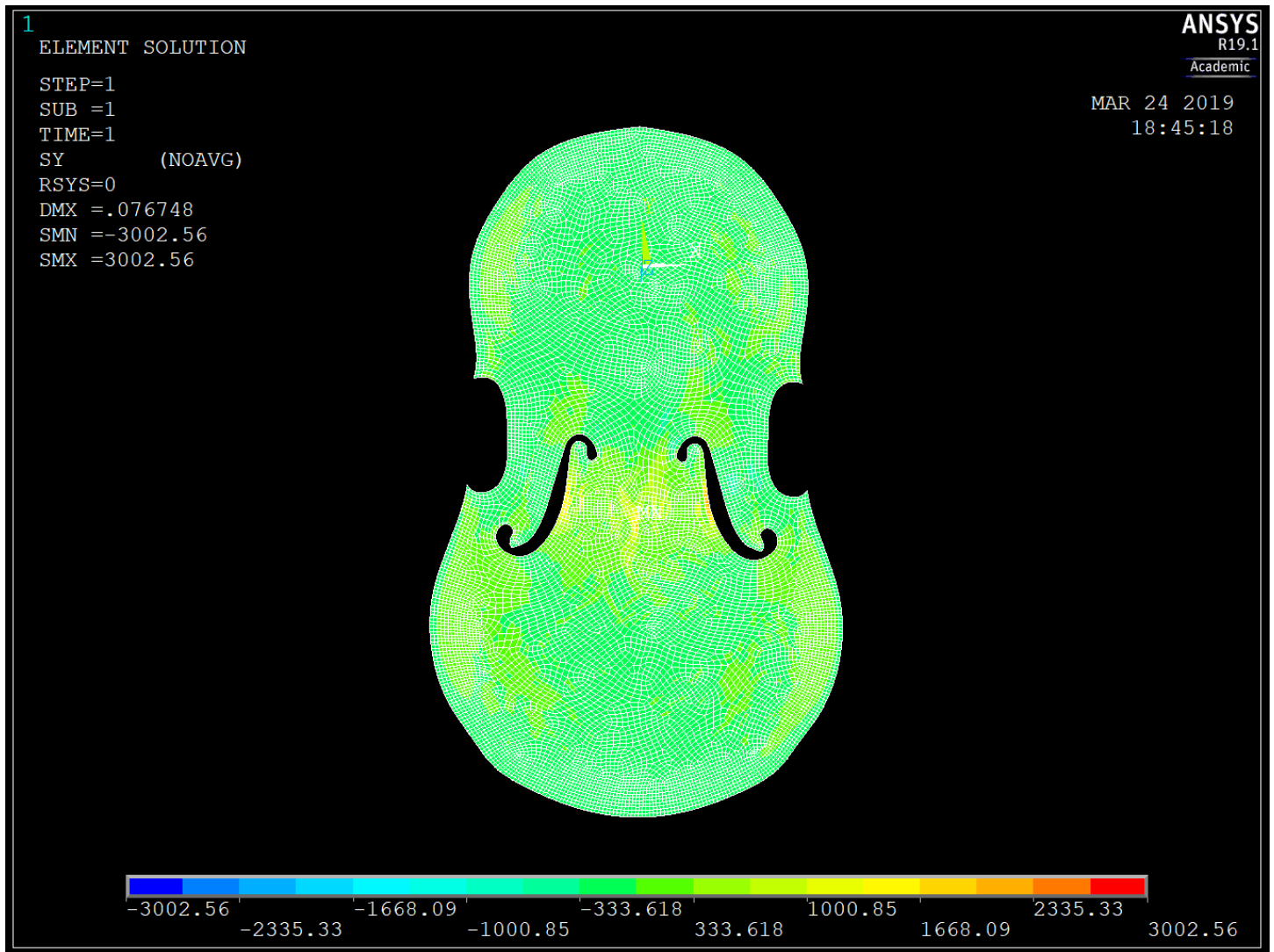


Figure 7: 1st Model Y-normal Stress Contour Plot

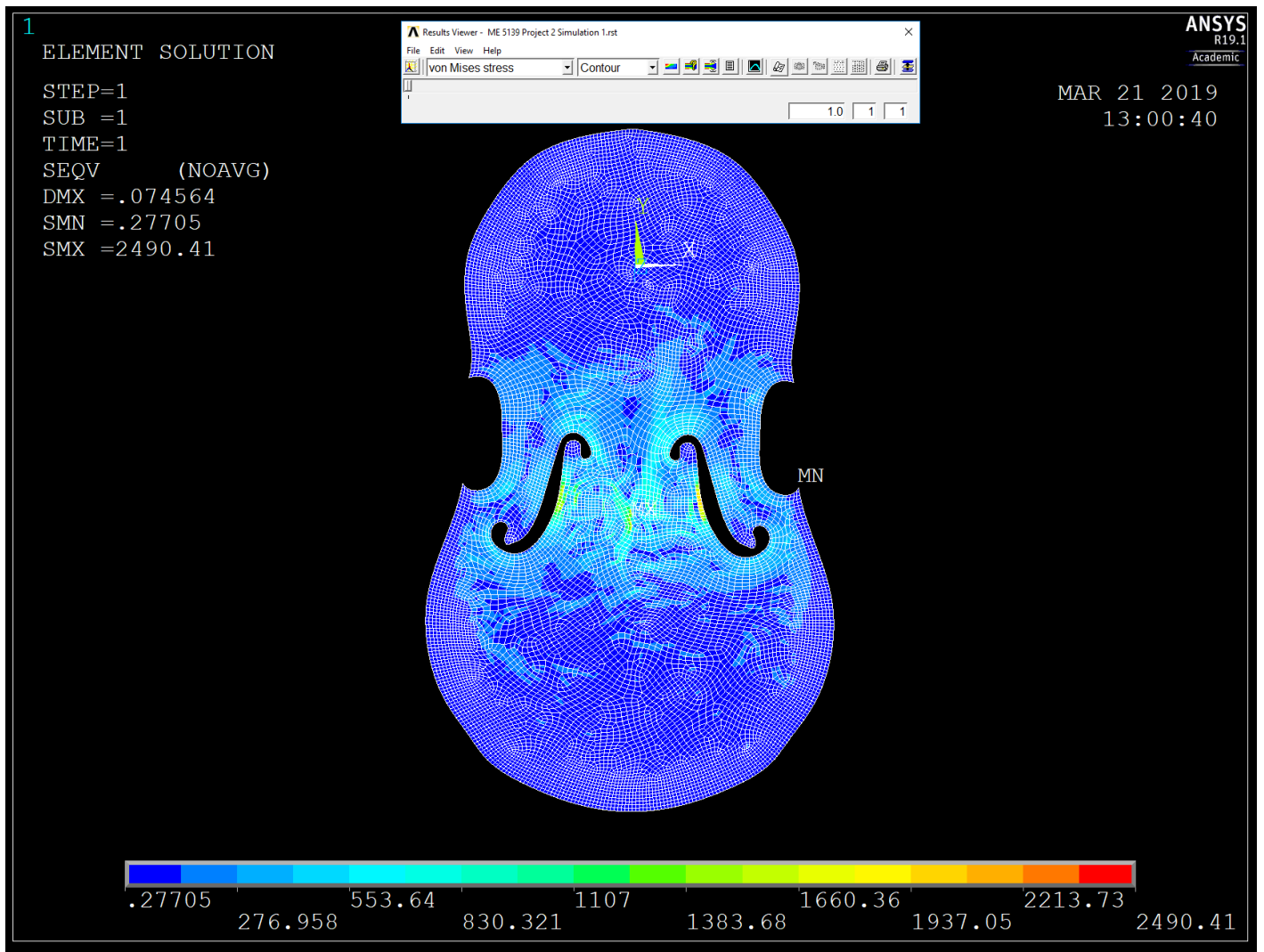


Figure 8: 1st Model von-Mises Stress Contour Plot

3. Structural Analysis for the Fourth Model

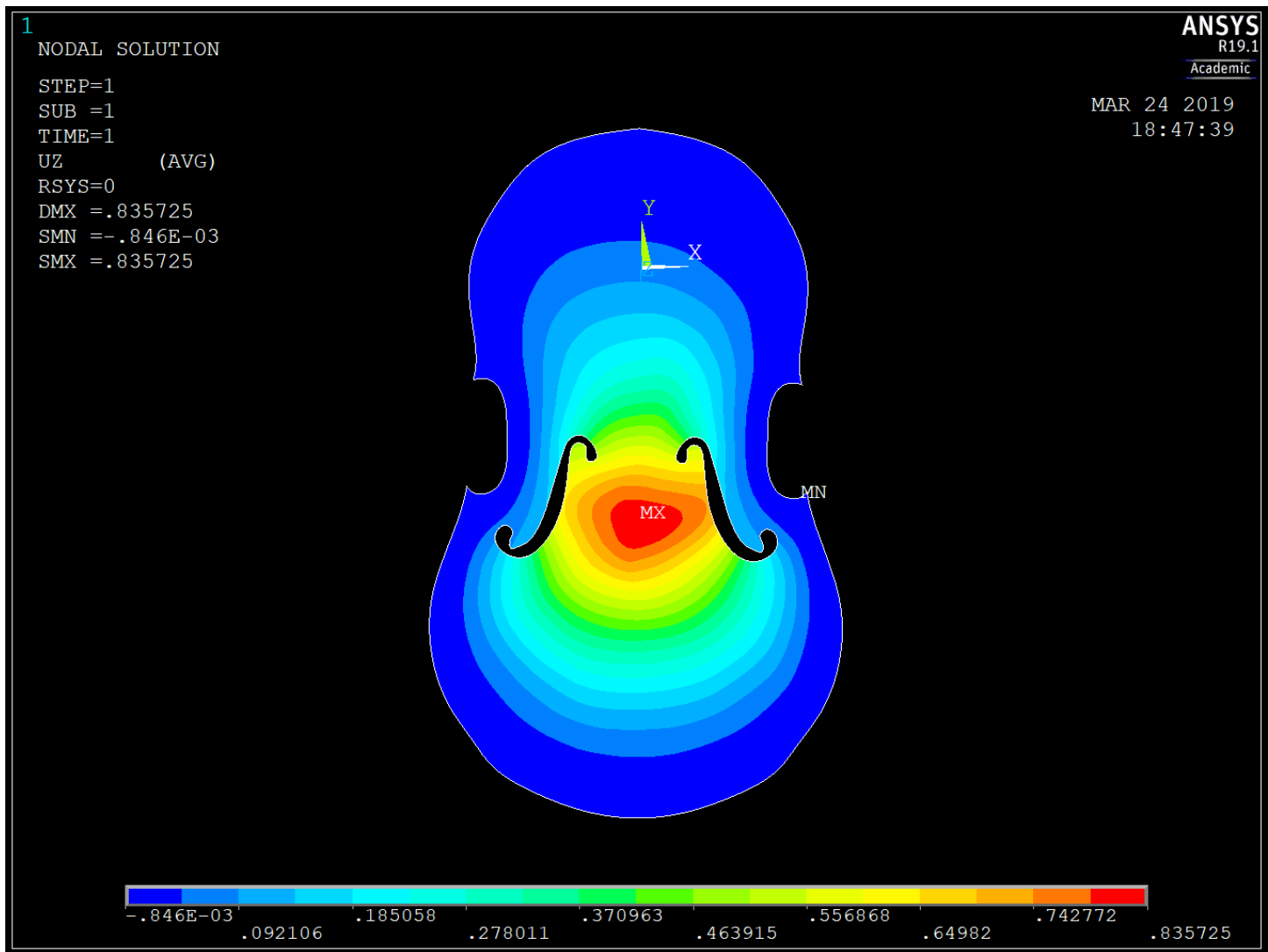


Figure 9: 4th Model Z-Displacement Contour Plot

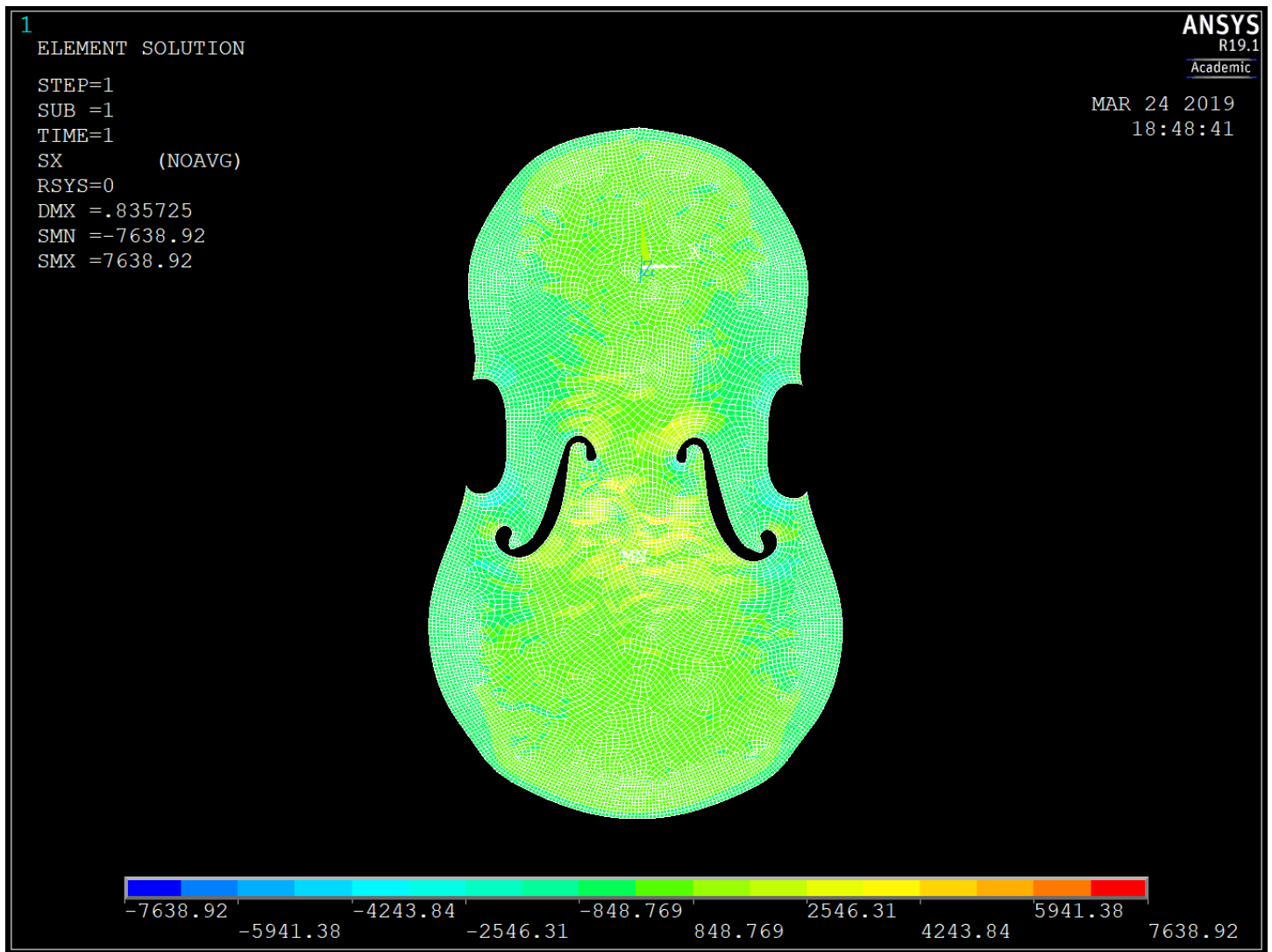


Figure 10: 4th Model X-normal Stress Contour Plot

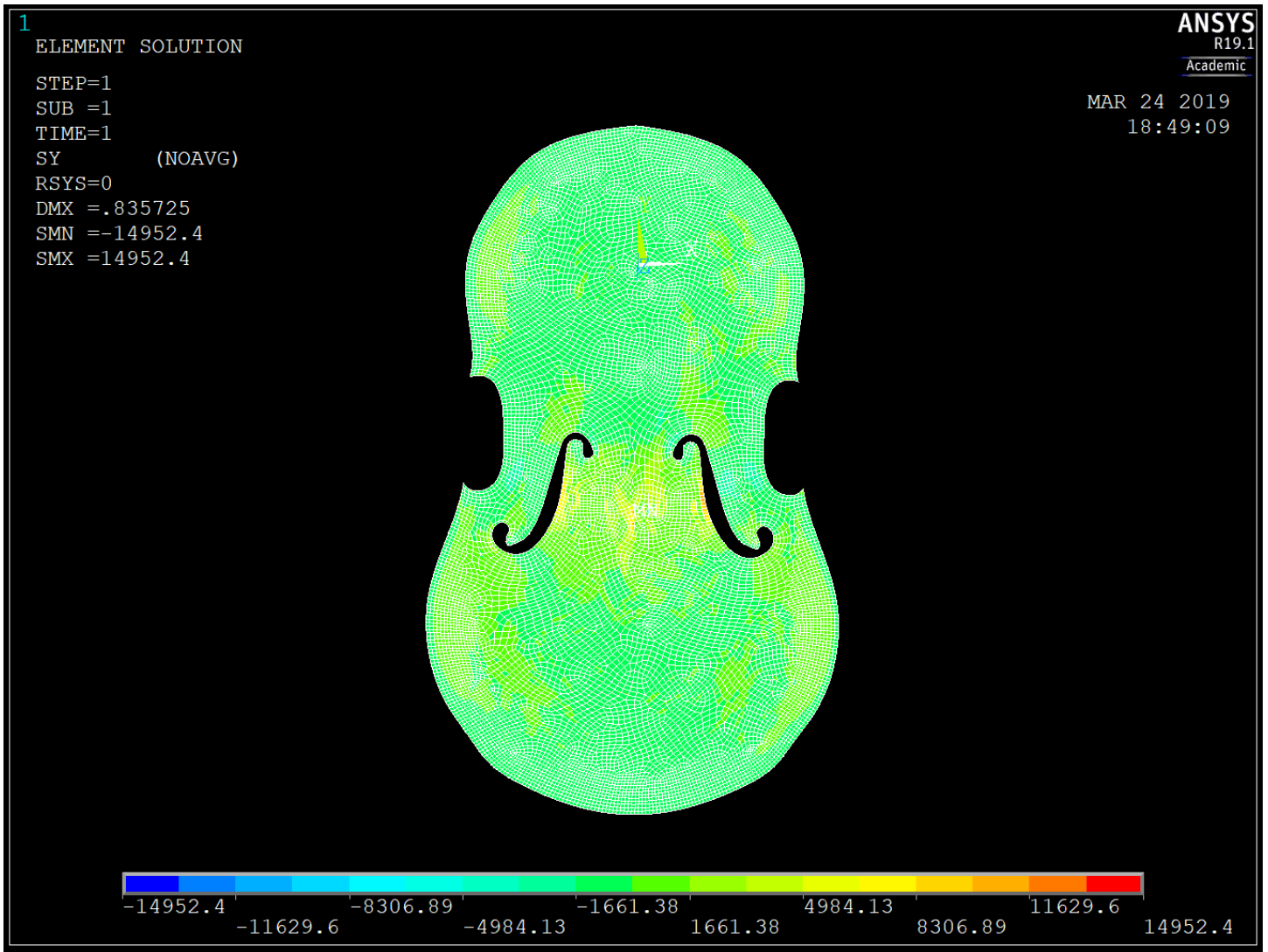


Figure 11: 4th Model Y-normal Stress Contour Plot

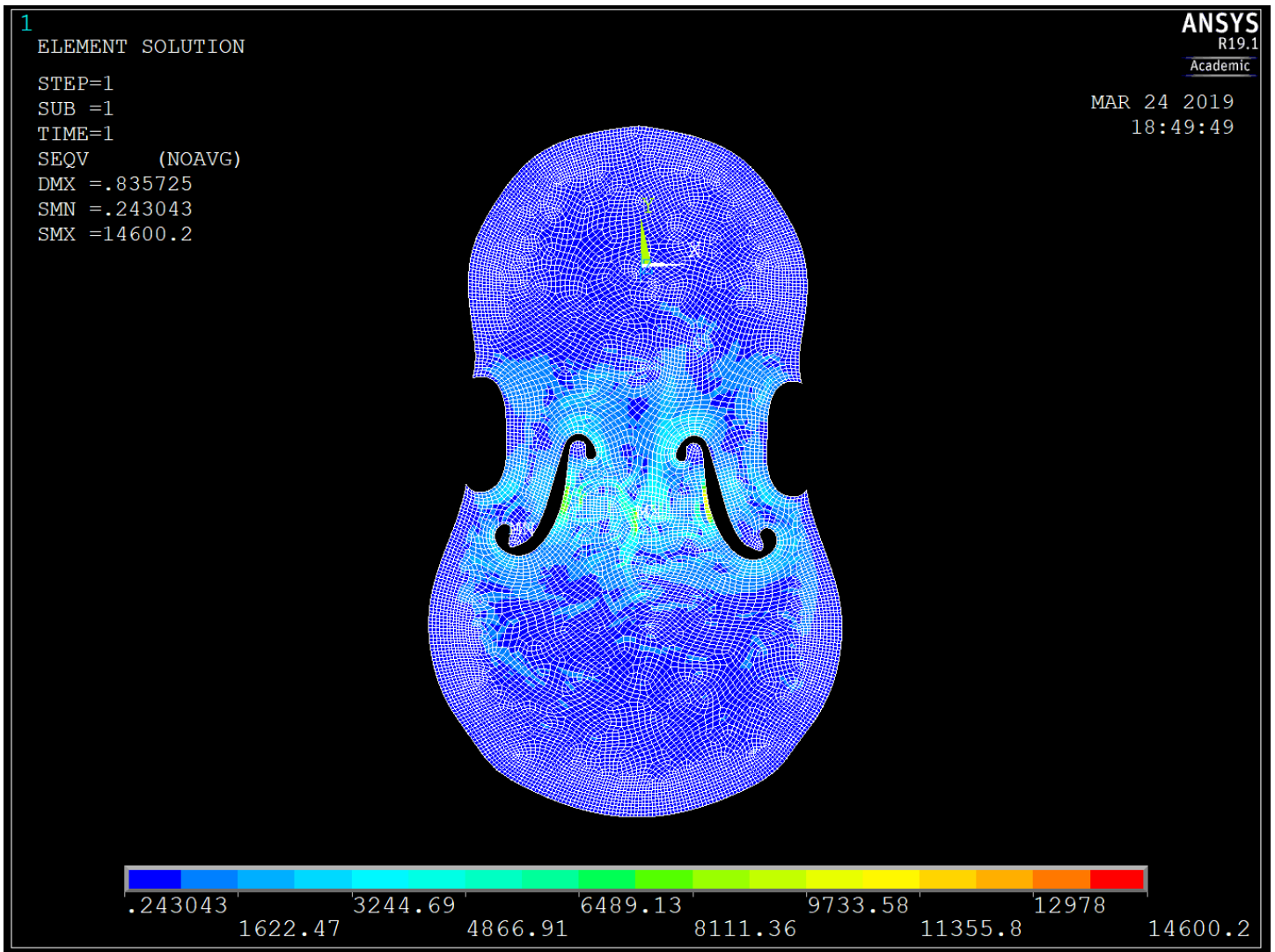
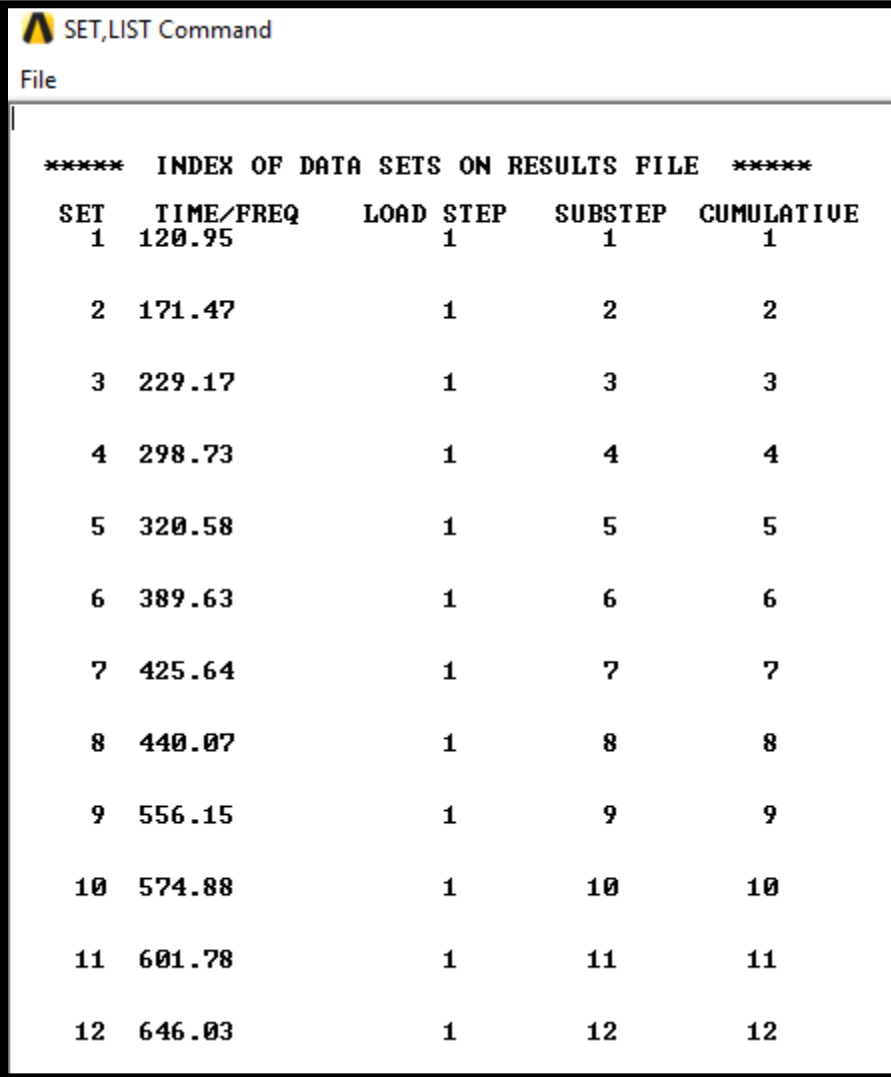


Figure 12: 4th Model von-Mises Stress Contour Plot

4. Model Analysis for the Second Model



SET,LIST Command

File

***** INDEX OF DATA SETS ON RESULTS FILE *****				
SET	TIME/FREQ	LOAD STEP	SUBSTEP	CUMULATIVE
1	120.95	1	1	1
2	171.47	1	2	2
3	229.17	1	3	3
4	298.73	1	4	4
5	320.58	1	5	5
6	389.63	1	6	6
7	425.64	1	7	7
8	440.07	1	8	8
9	556.15	1	9	9
10	574.88	1	10	10
11	601.78	1	11	11
12	646.03	1	12	12

Figure 13: 2nd Model Natural Frequency with Different Modes

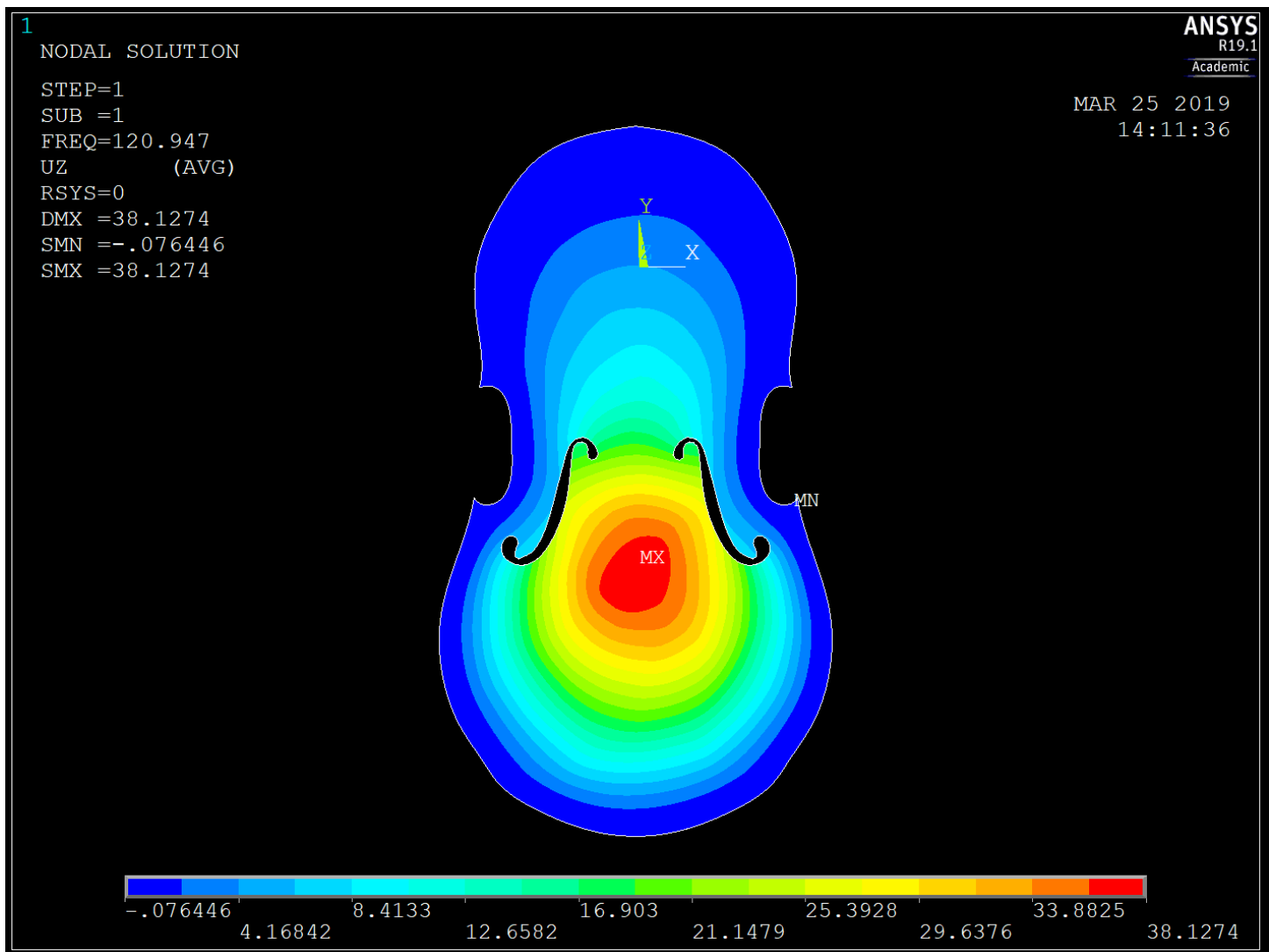


Figure 14: 2nd Model Mode 1 Natural Frequency Z-Displacement Contour Plot

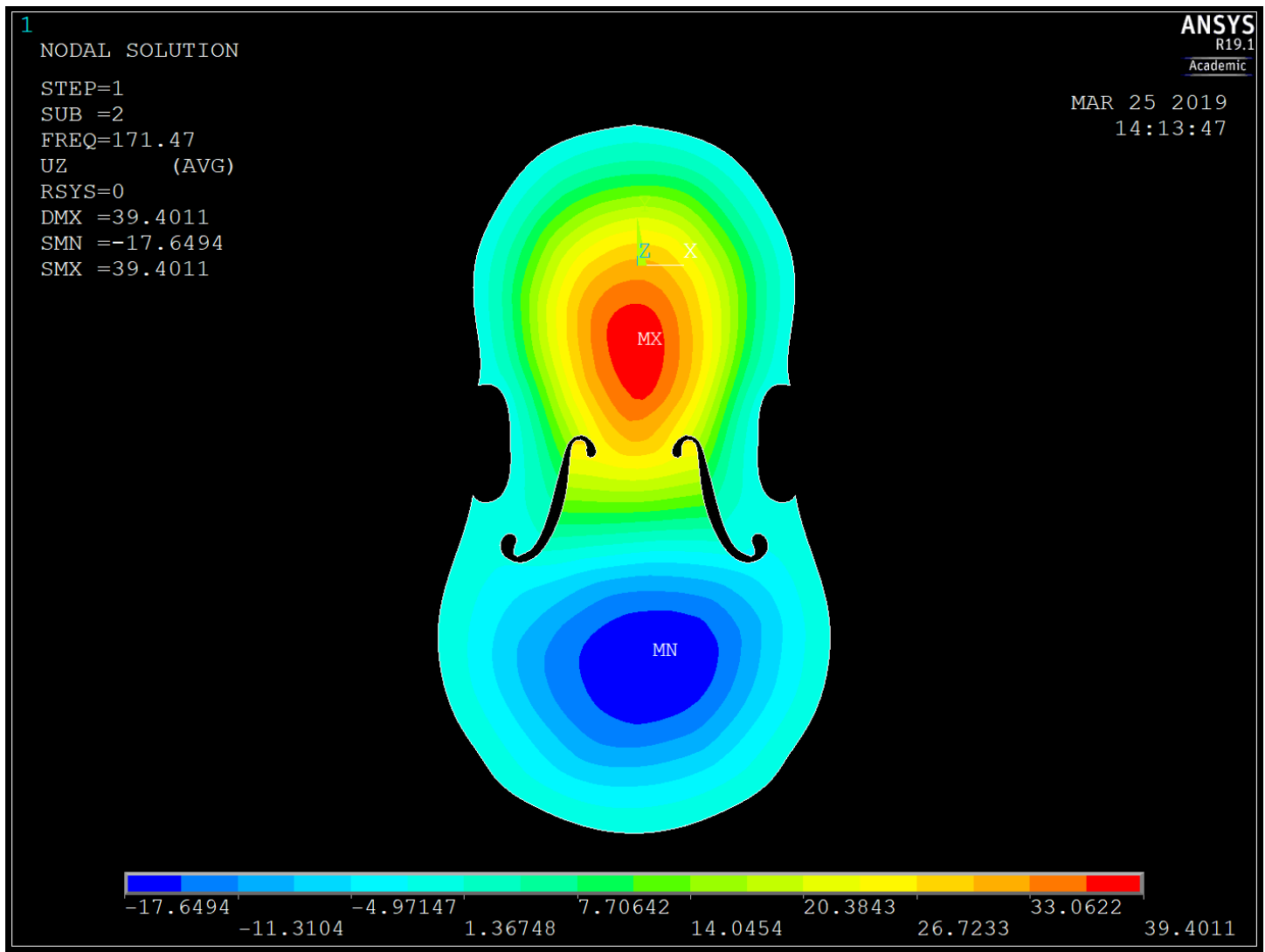


Figure 15: 2nd Model Mode 2 Natural Frequency Z-Displacement Contour Plot

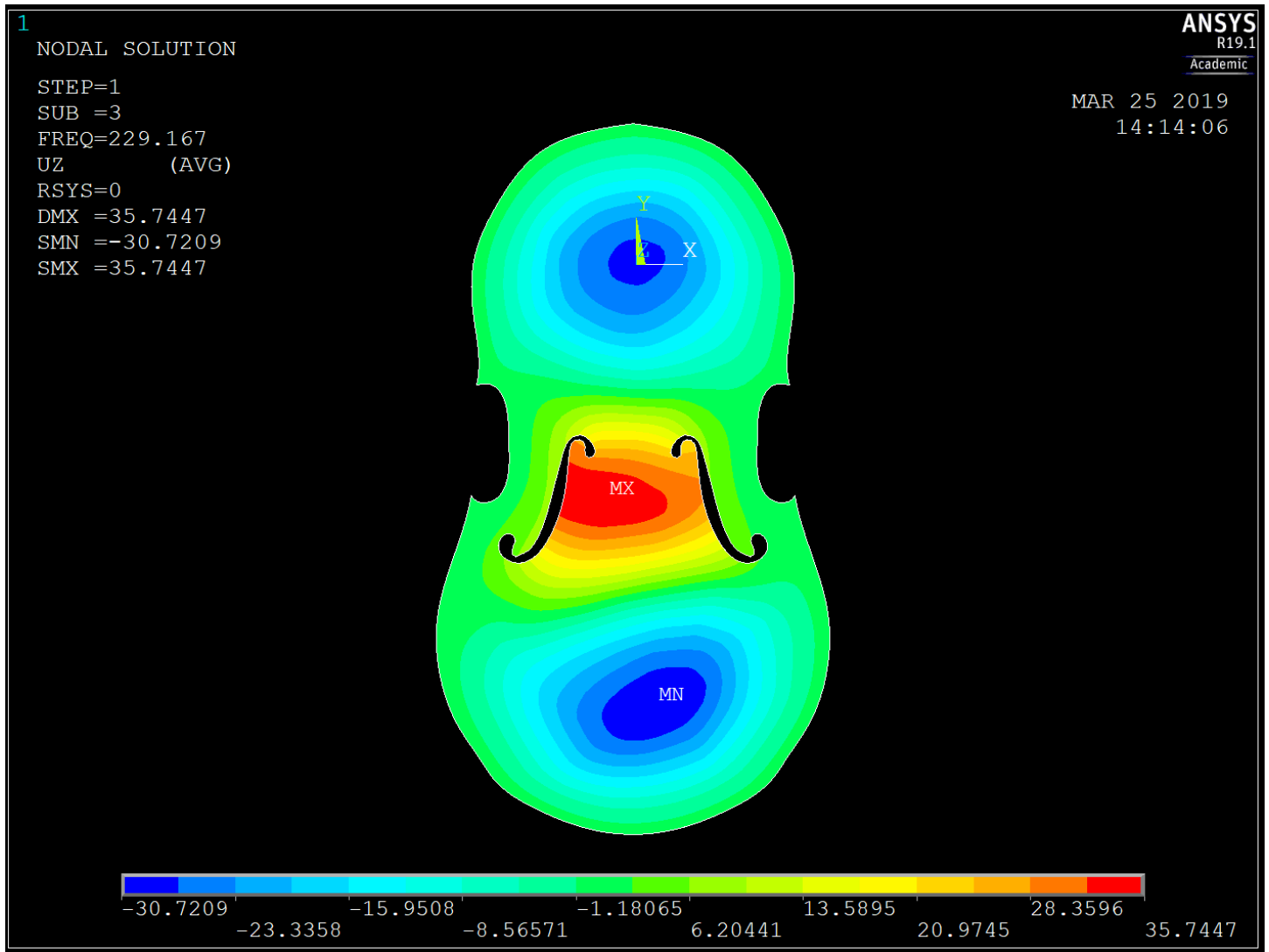


Figure 16: 2nd Model Mode 3 Natural Frequency Z-Displacement Contour Plot



Figure 17: 2nd Model Mode 4 Natural Frequency Z-Displacement Contour Plot

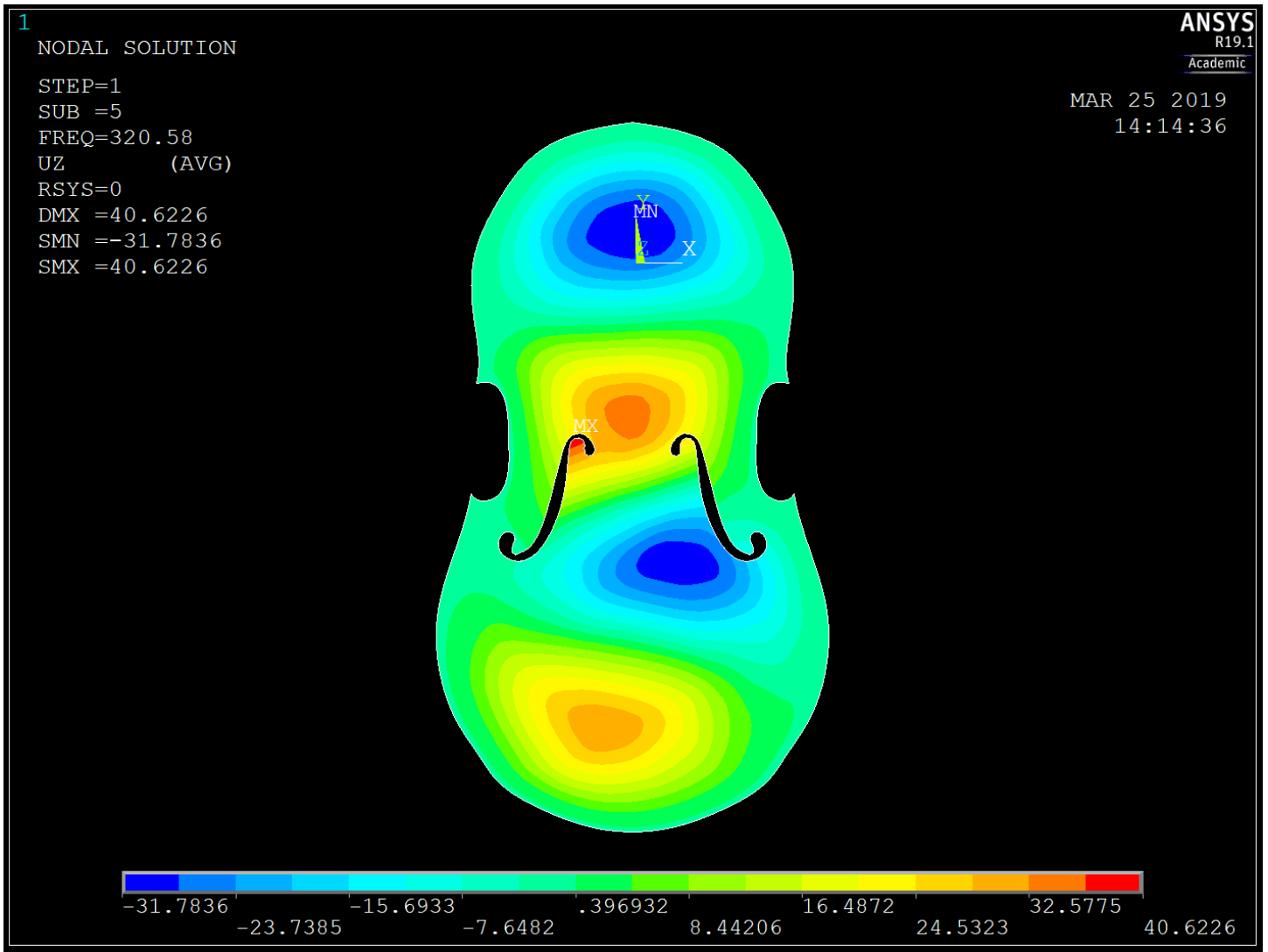


Figure 18: 2nd Model Mode 5 Natural Frequency Z-Displacement Contour Plot

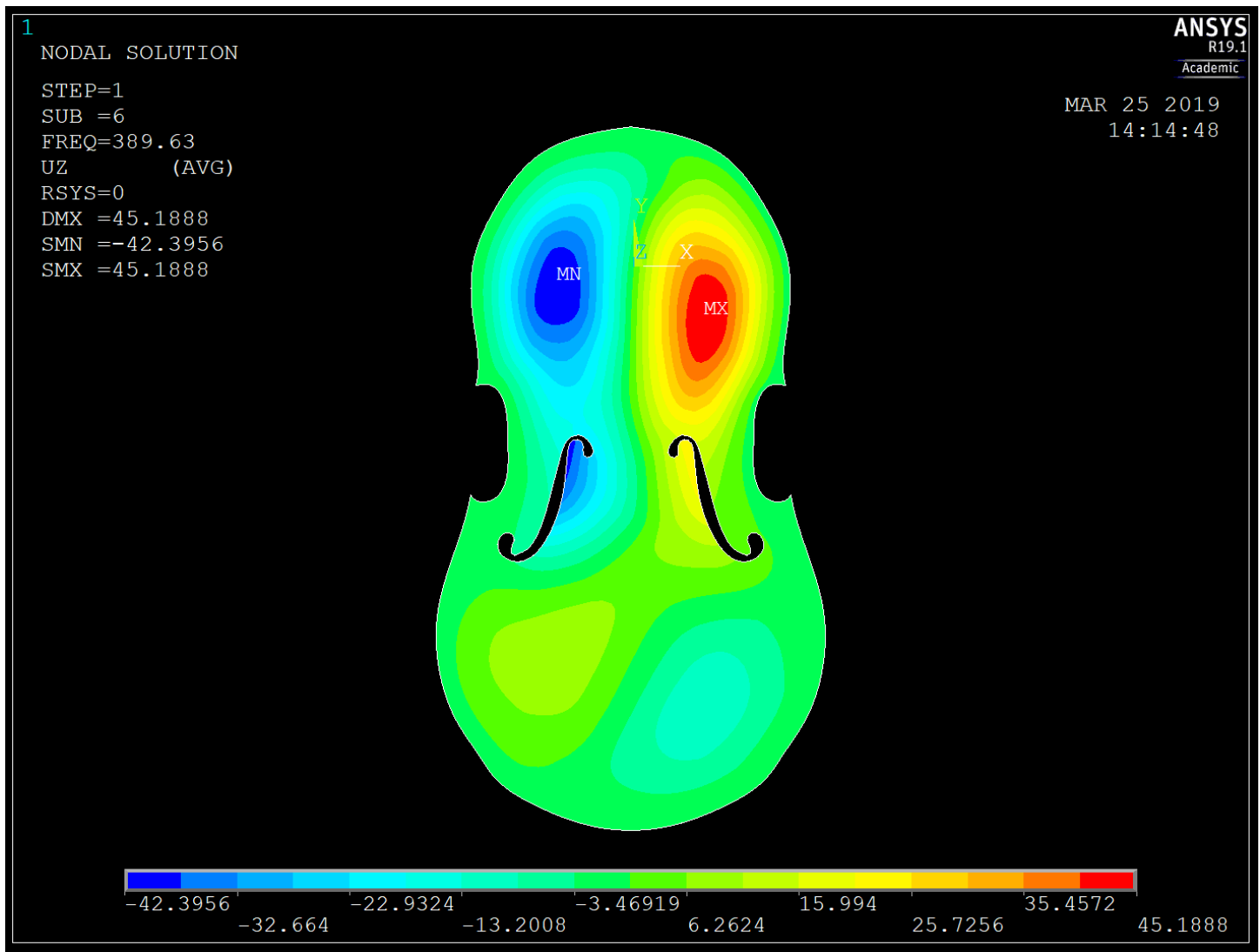


Figure 19: 2nd Model Mode 6 Natural Frequency Z-Displacement Contour Plot

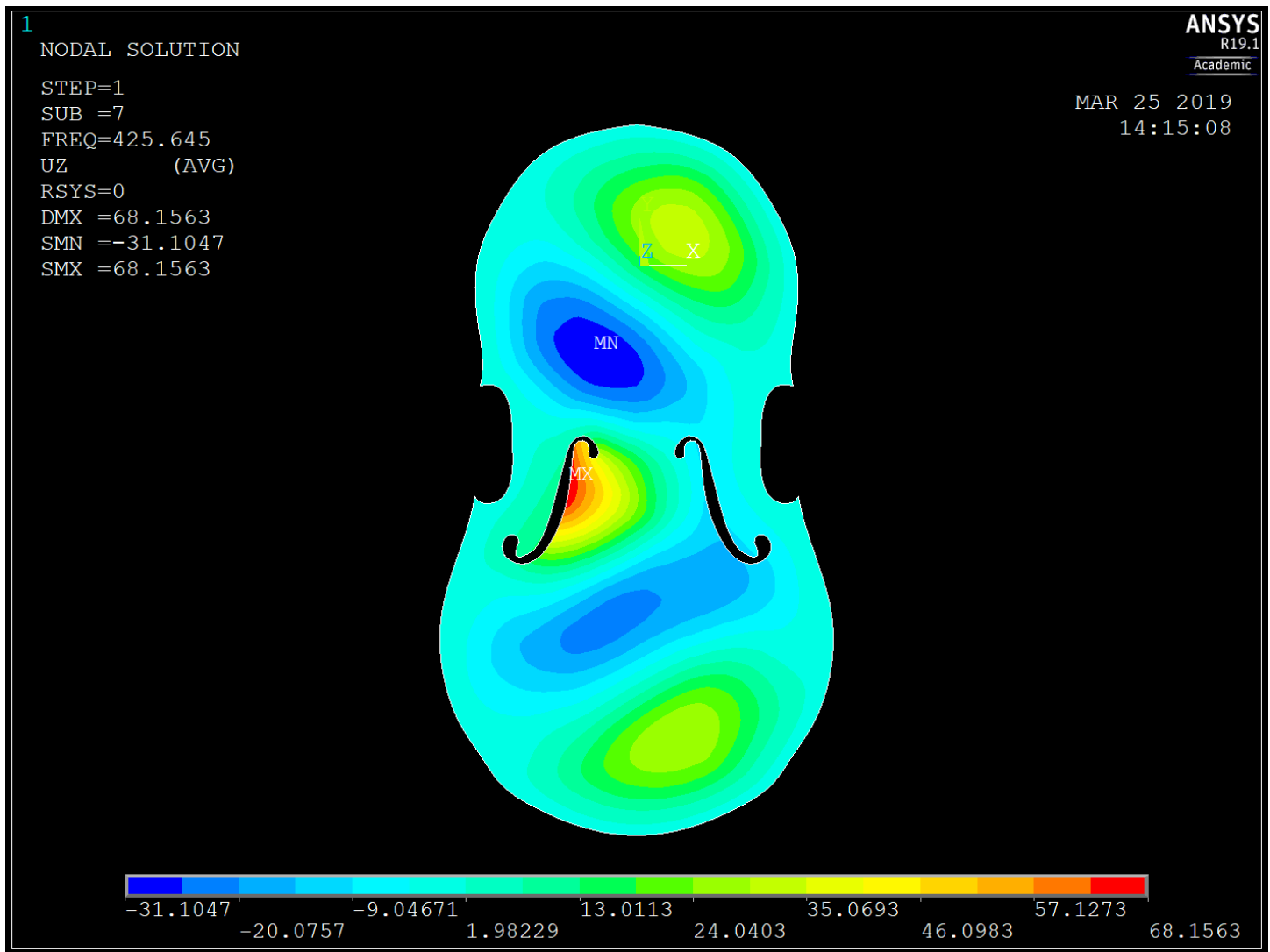
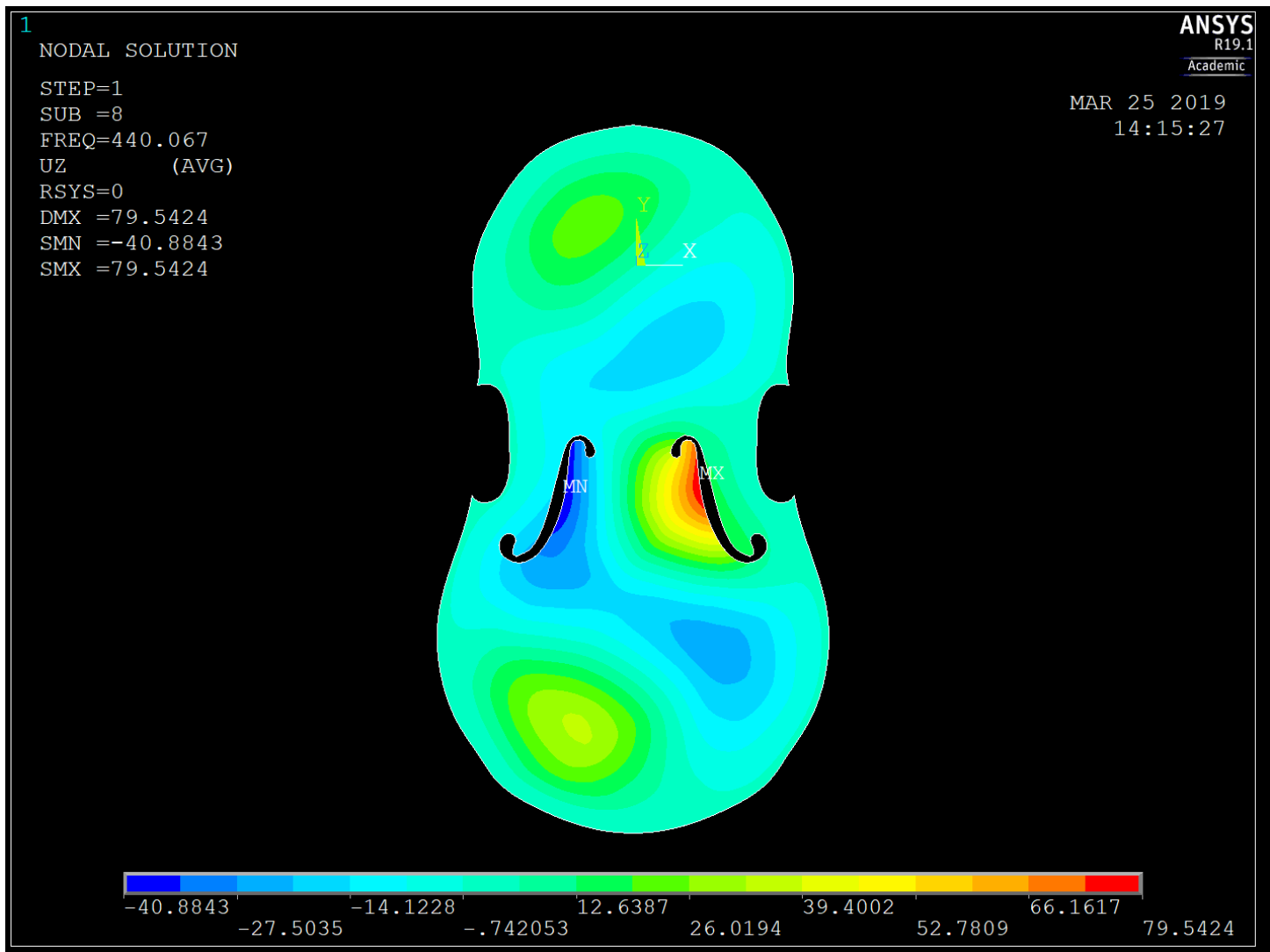


Figure 20: 2nd Model Mode 7 Natural Frequency Z-Displacement Contour Plot



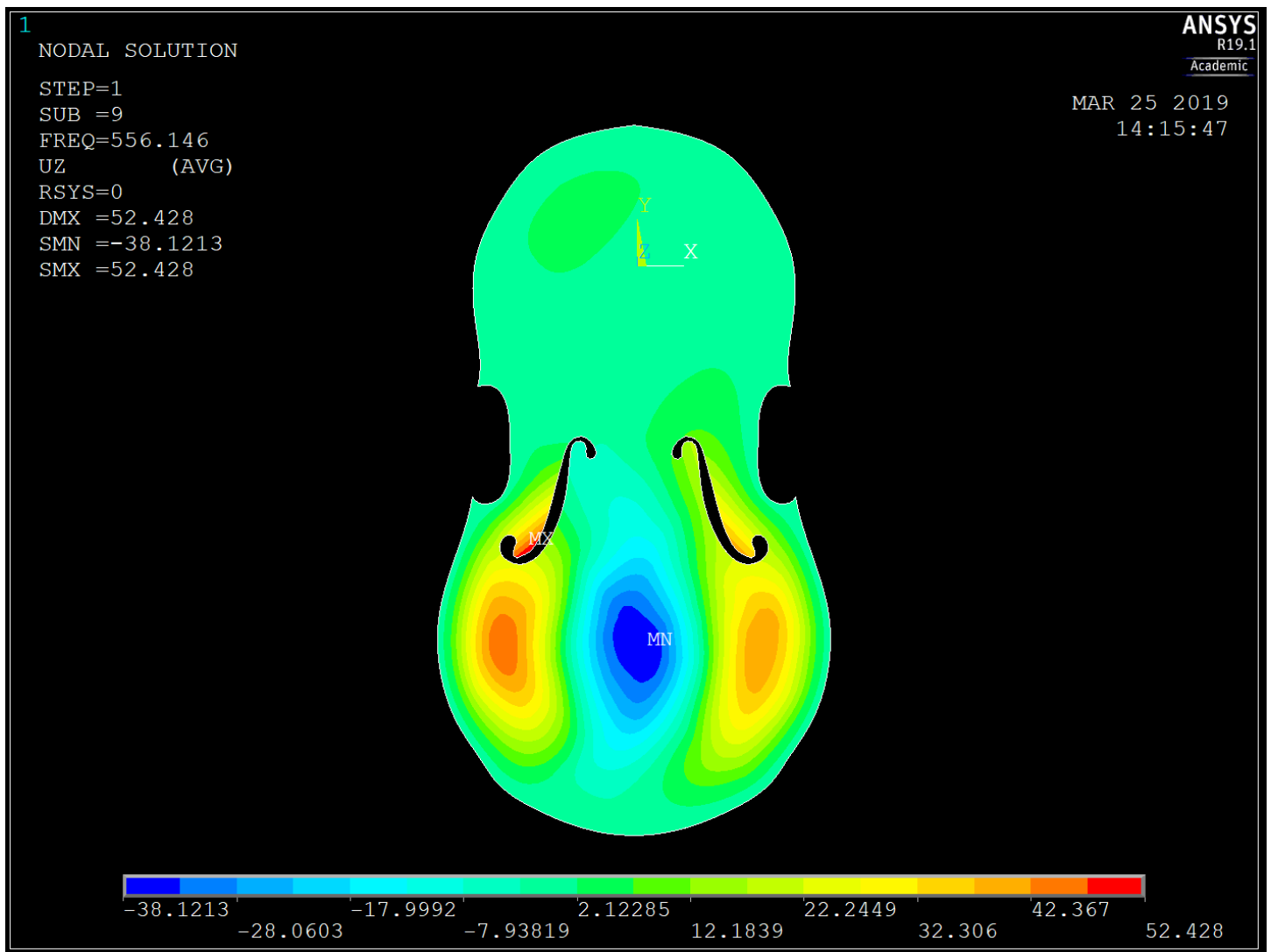


Figure 22: 2nd Model Mode 9 Natural Frequency Z-Displacement Contour Plot

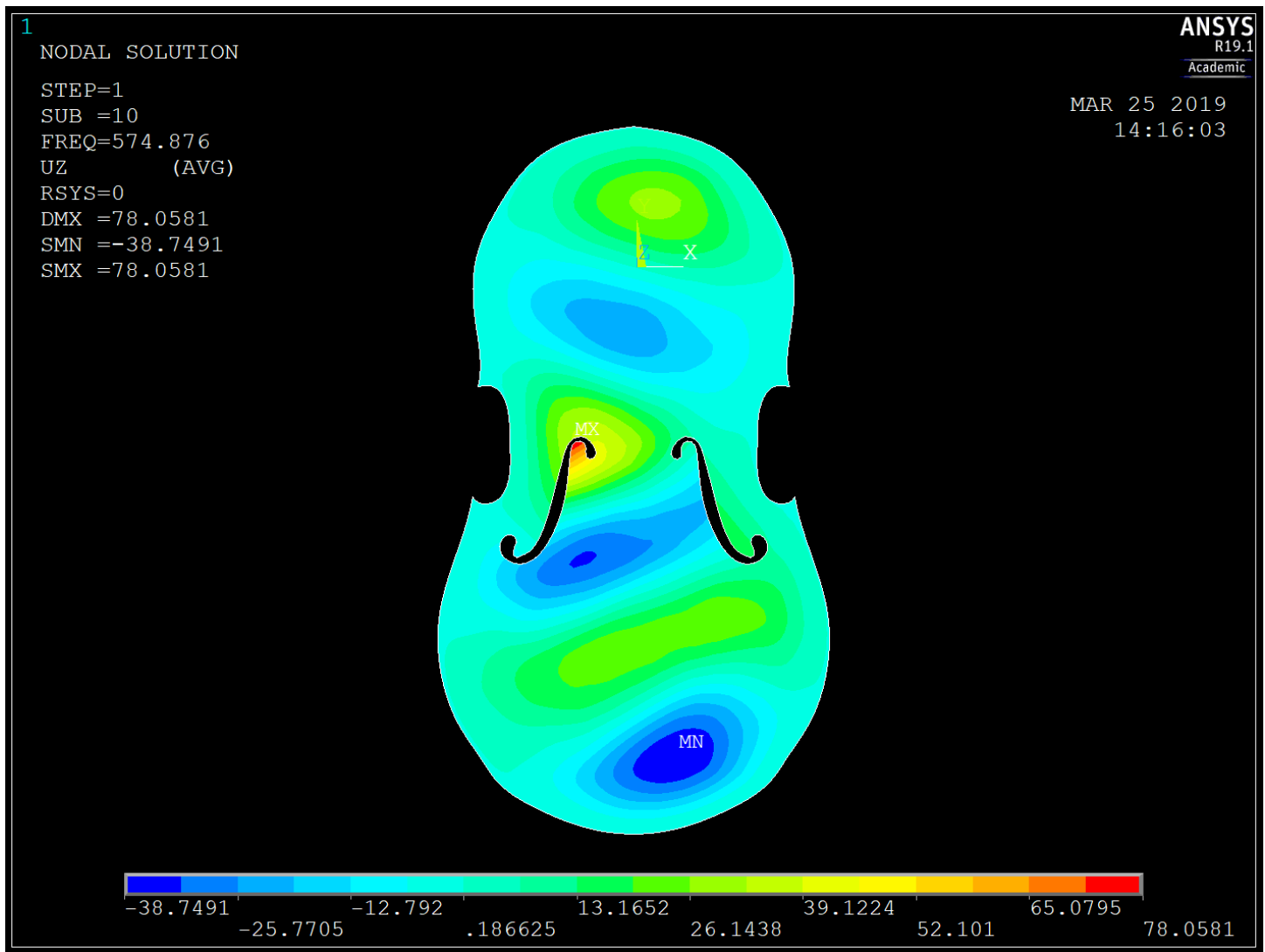


Figure 23: 2nd Model Mode 10 Natural Frequency Z-Displacement Contour Plot

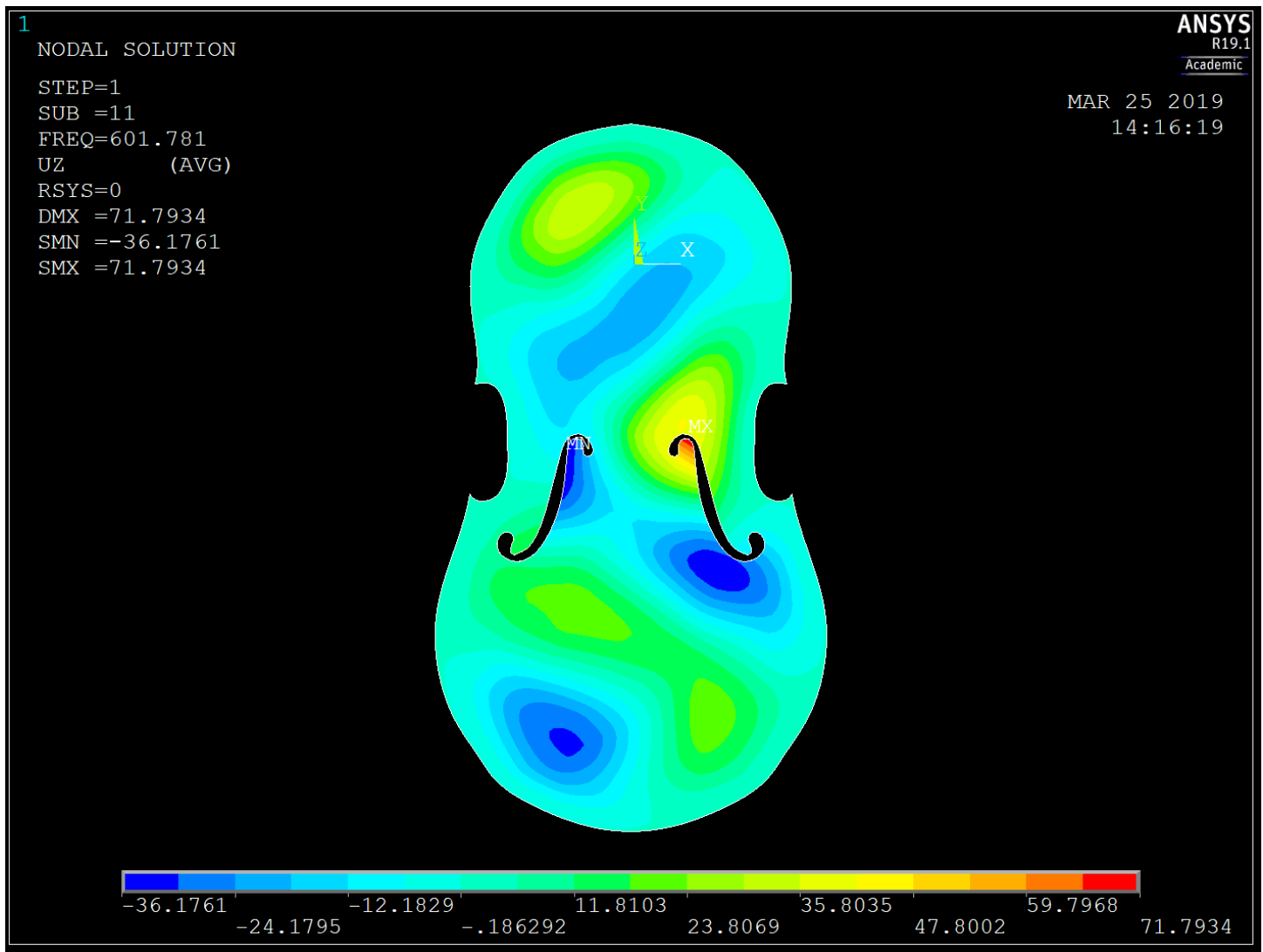


Figure 24: 2nd Model Mode 11 Natural Frequency Z-Displacement Contour Plot

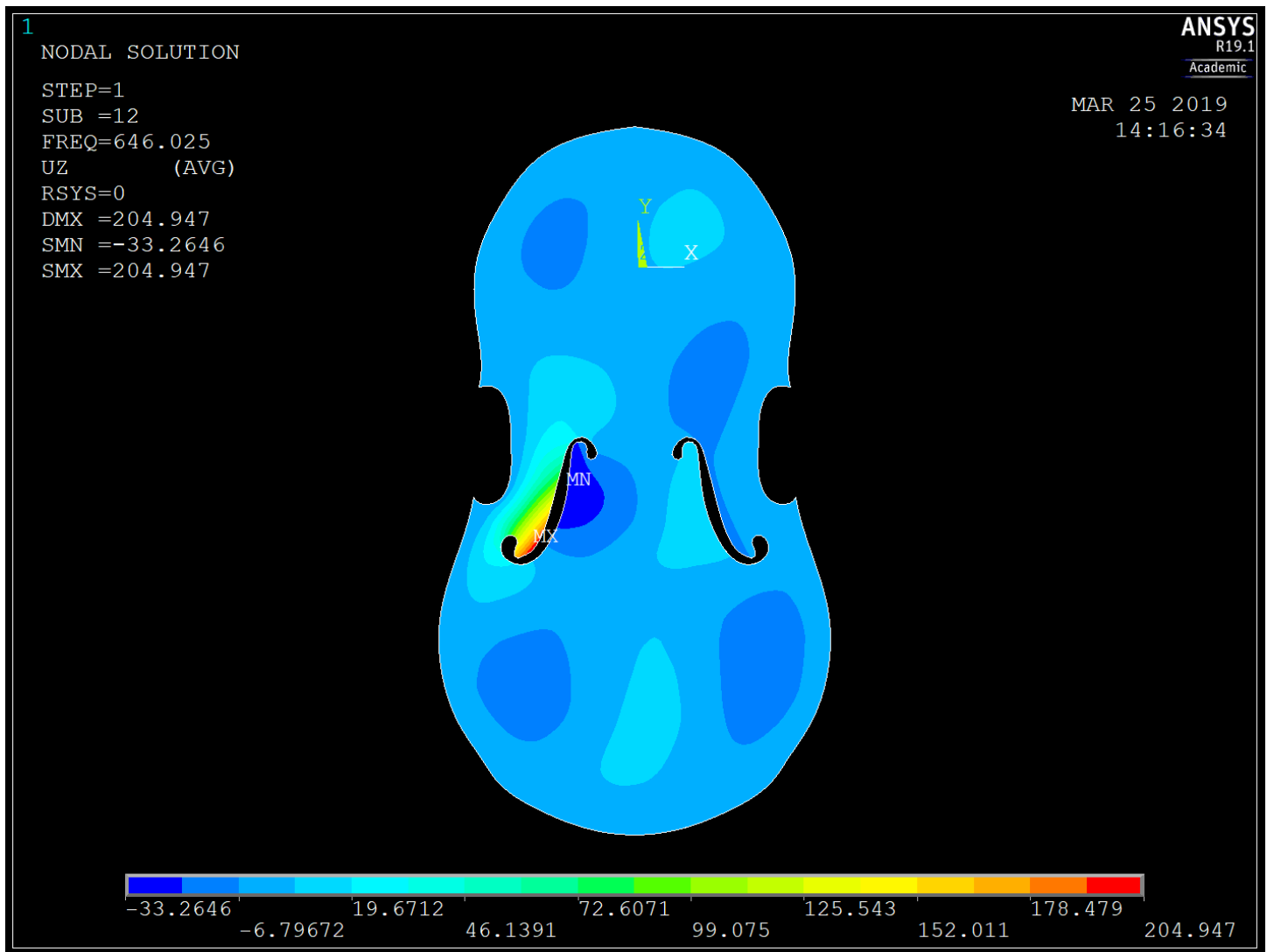
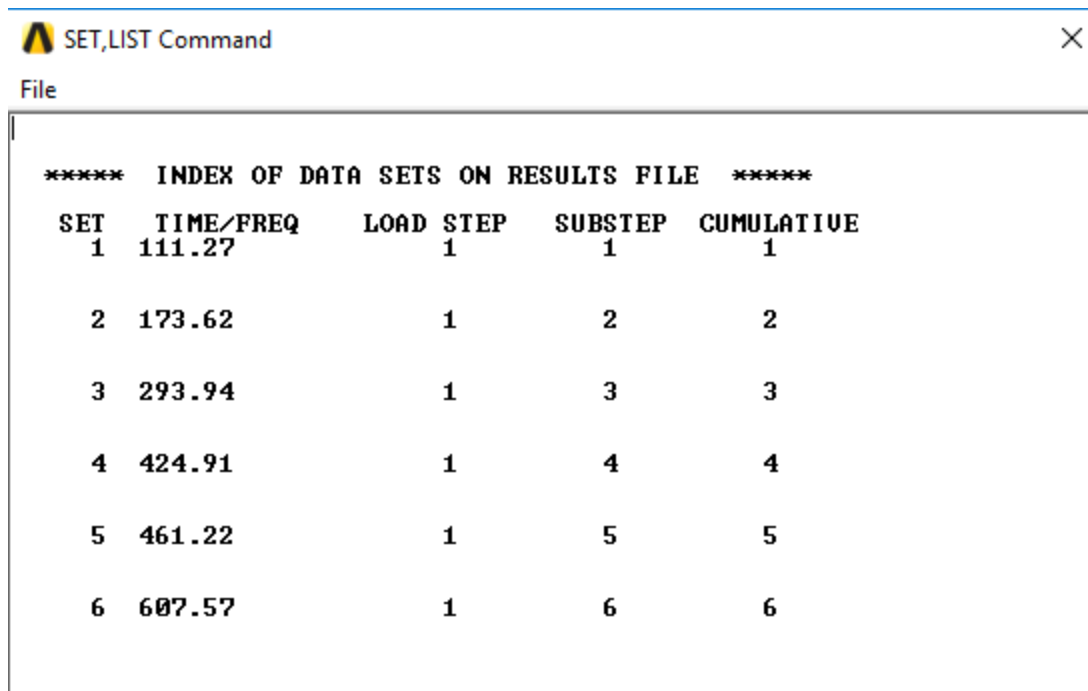


Figure 25: 2nd Model Mode 12 Natural Frequency Z-Displacement Contour Plot

5. Model Analysis for the Third Model



SET,LIST Command

File

***** INDEX OF DATA SETS ON RESULTS FILE *****				
SET	TIME/FREQ	LOAD STEP	SUBSTEP	CUMULATIVE
1	111.27	1	1	1
2	173.62	1	2	2
3	293.94	1	3	3
4	424.91	1	4	4
5	461.22	1	5	5
6	607.57	1	6	6

Figure 26: 3rd Model Natural Frequency with Different Modes

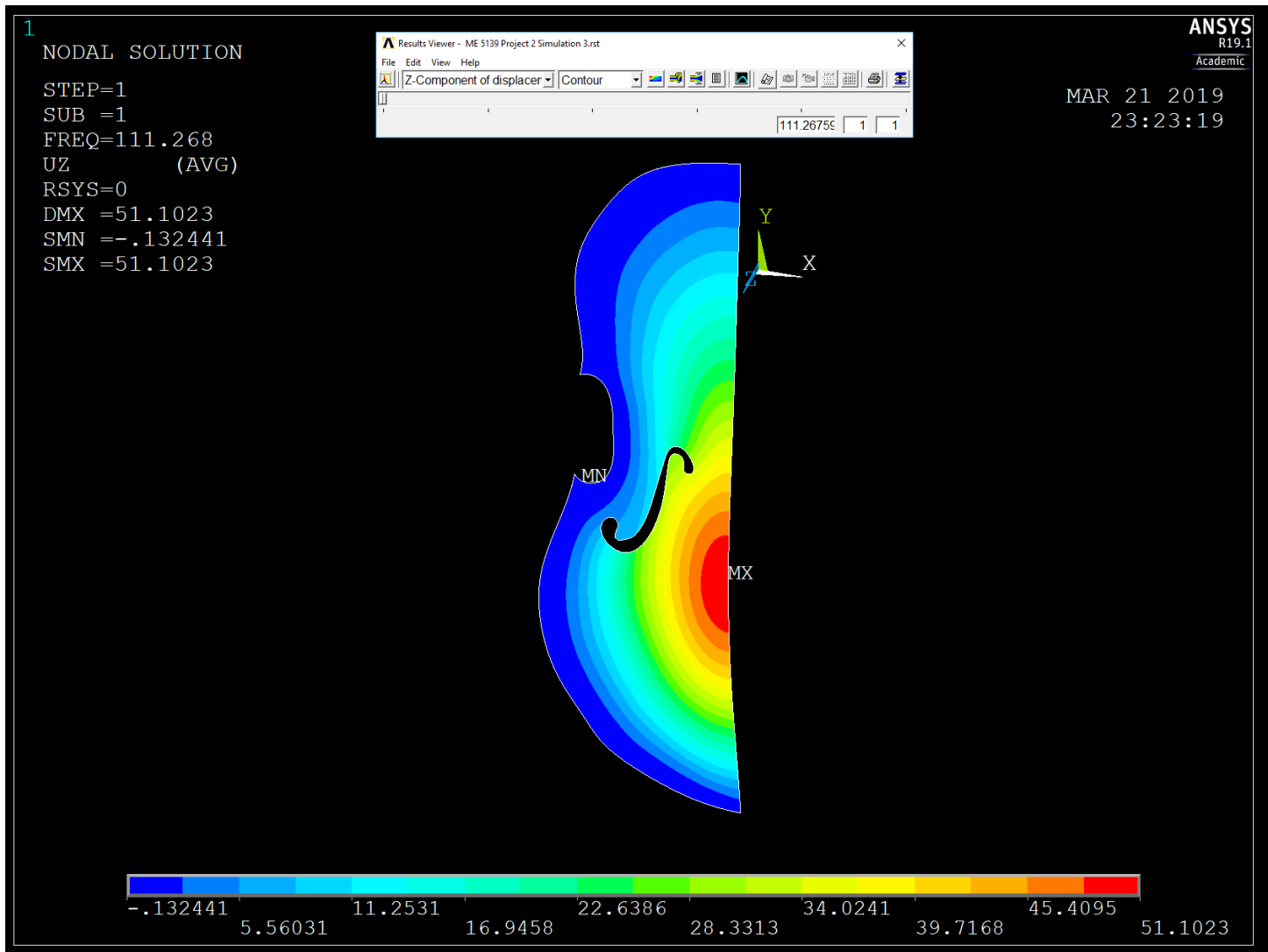


Figure 27: 3rd Model Mode 1 Natural Frequency Z-Displacement Contour Plot

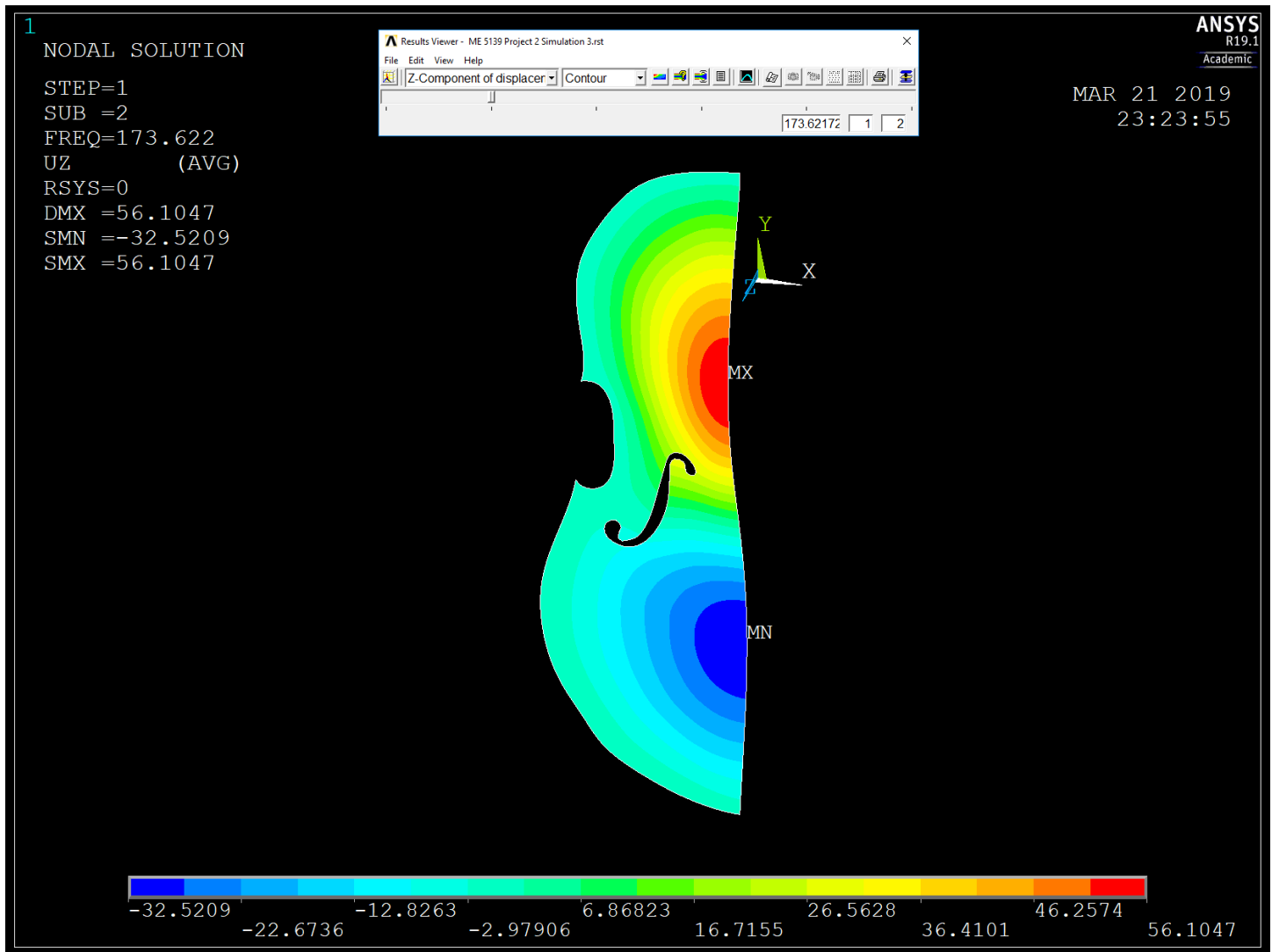


Figure 28: 3rd Model Mode 2 Natural Frequency Z-Displacement Contour Plot

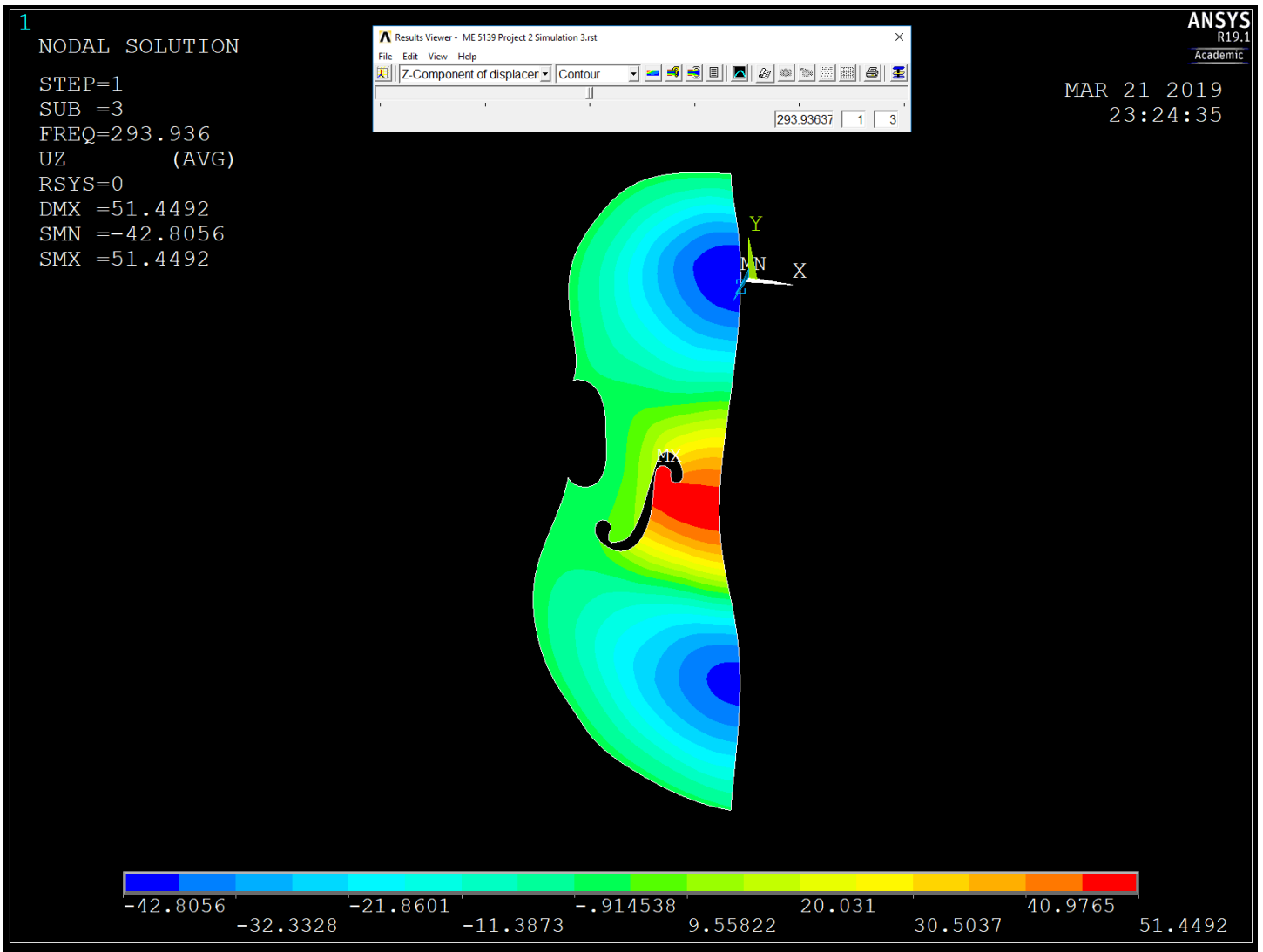


Figure 29: 3rd Model Mode 3 Natural Frequency Z-Displacement Contour Plot

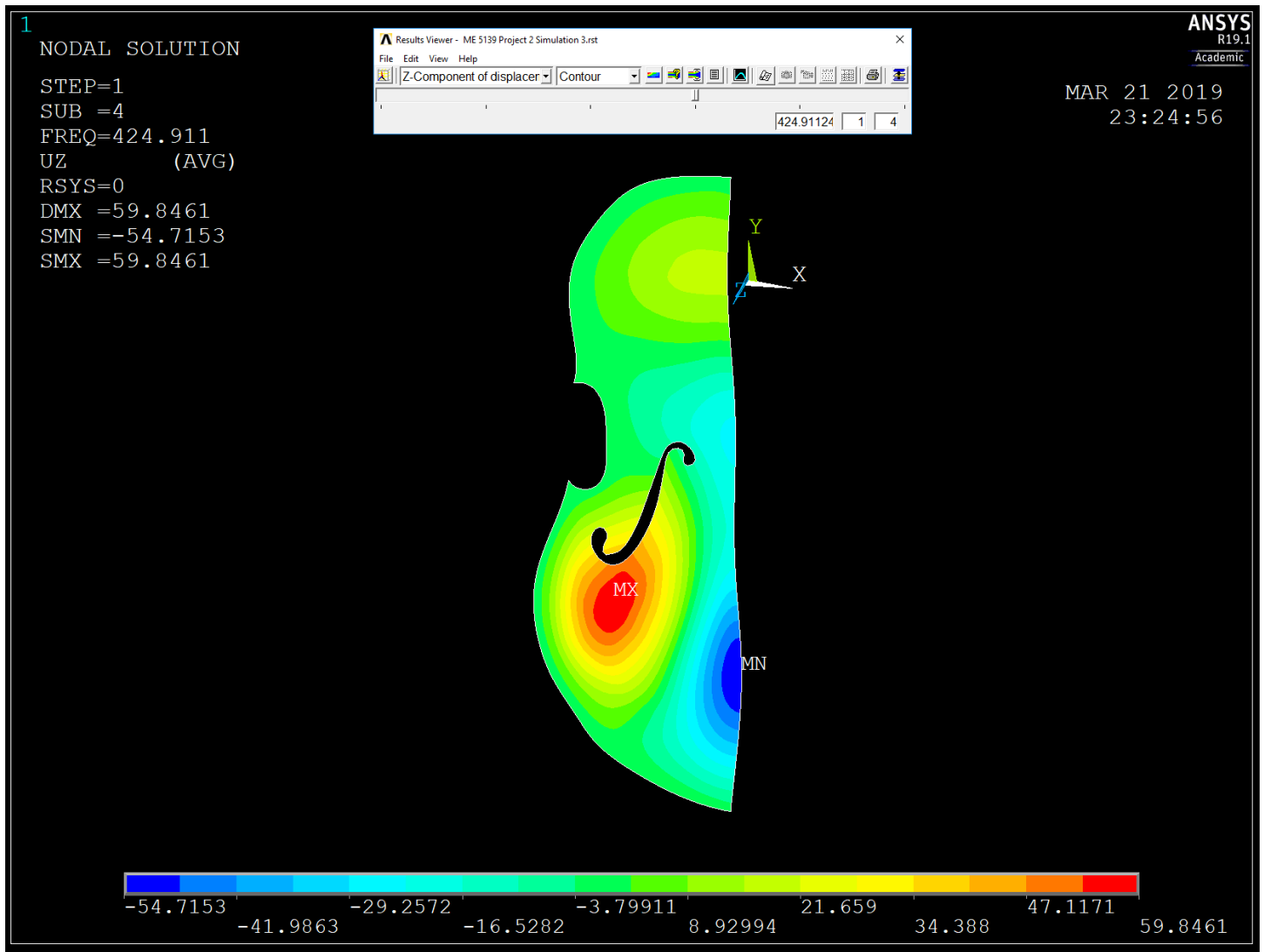


Figure 30: 3rd Model Mode 4 Natural Frequency Z-Displacement Contour Plot

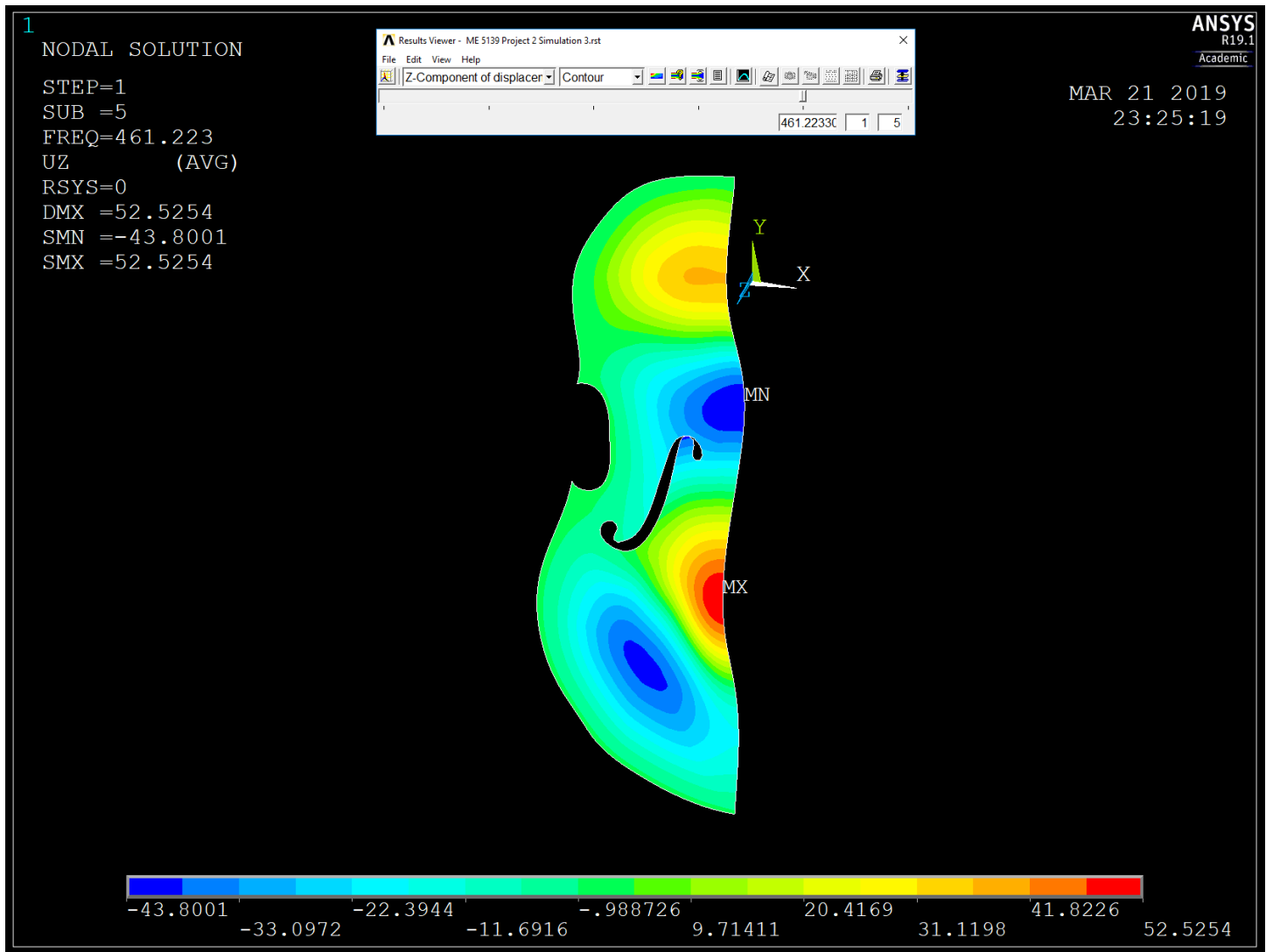


Figure 31: 3rd Model Mode 5 Natural Frequency Z-Displacement Contour Plot

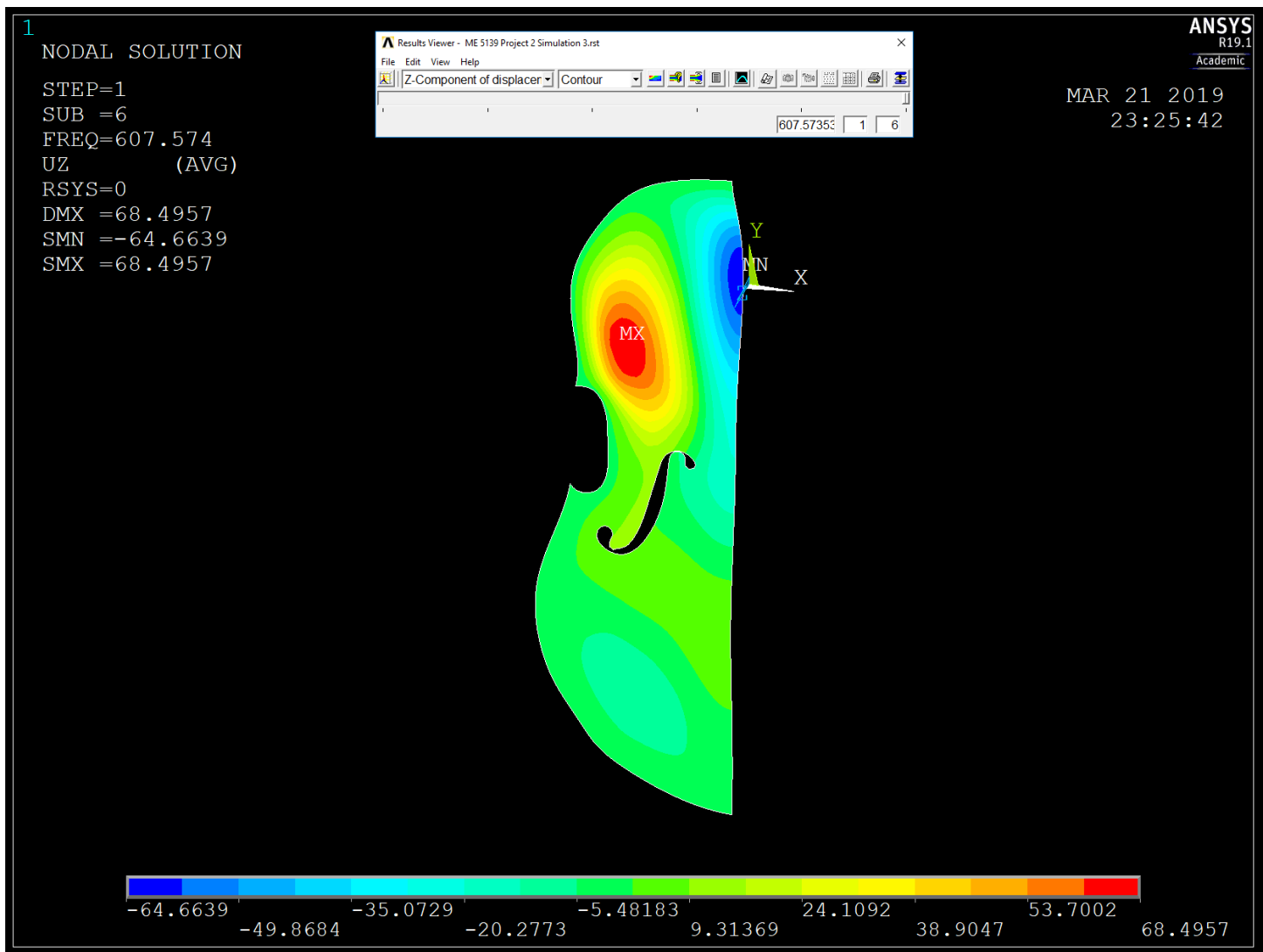
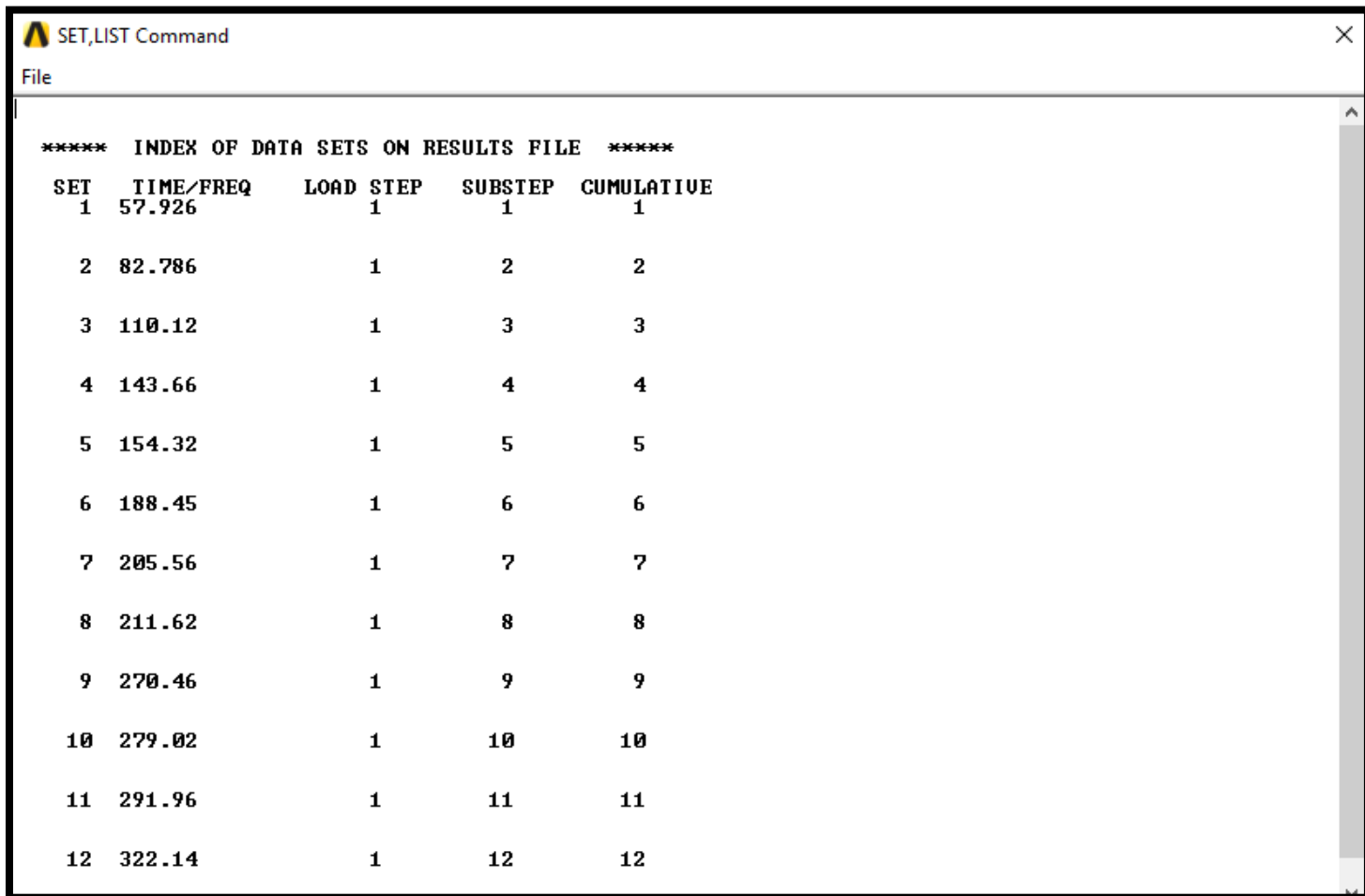


Figure 32: 3rd Model Mode 6 Natural Frequency Z-Displacement Contour Plot

6. Model Analysis for the Fifth Model



SET,LIST Command

File

***** INDEX OF DATA SETS ON RESULTS FILE *****

SET	TIME/FREQ	LOAD STEP	SUBSTEP	CUMULATIVE
1	57.926	1	1	1
2	82.786	1	2	2
3	110.12	1	3	3
4	143.66	1	4	4
5	154.32	1	5	5
6	188.45	1	6	6
7	205.56	1	7	7
8	211.62	1	8	8
9	270.46	1	9	9
10	279.02	1	10	10
11	291.96	1	11	11
12	322.14	1	12	12

Figure 33: 5th Model Natural Frequency with Different Modes

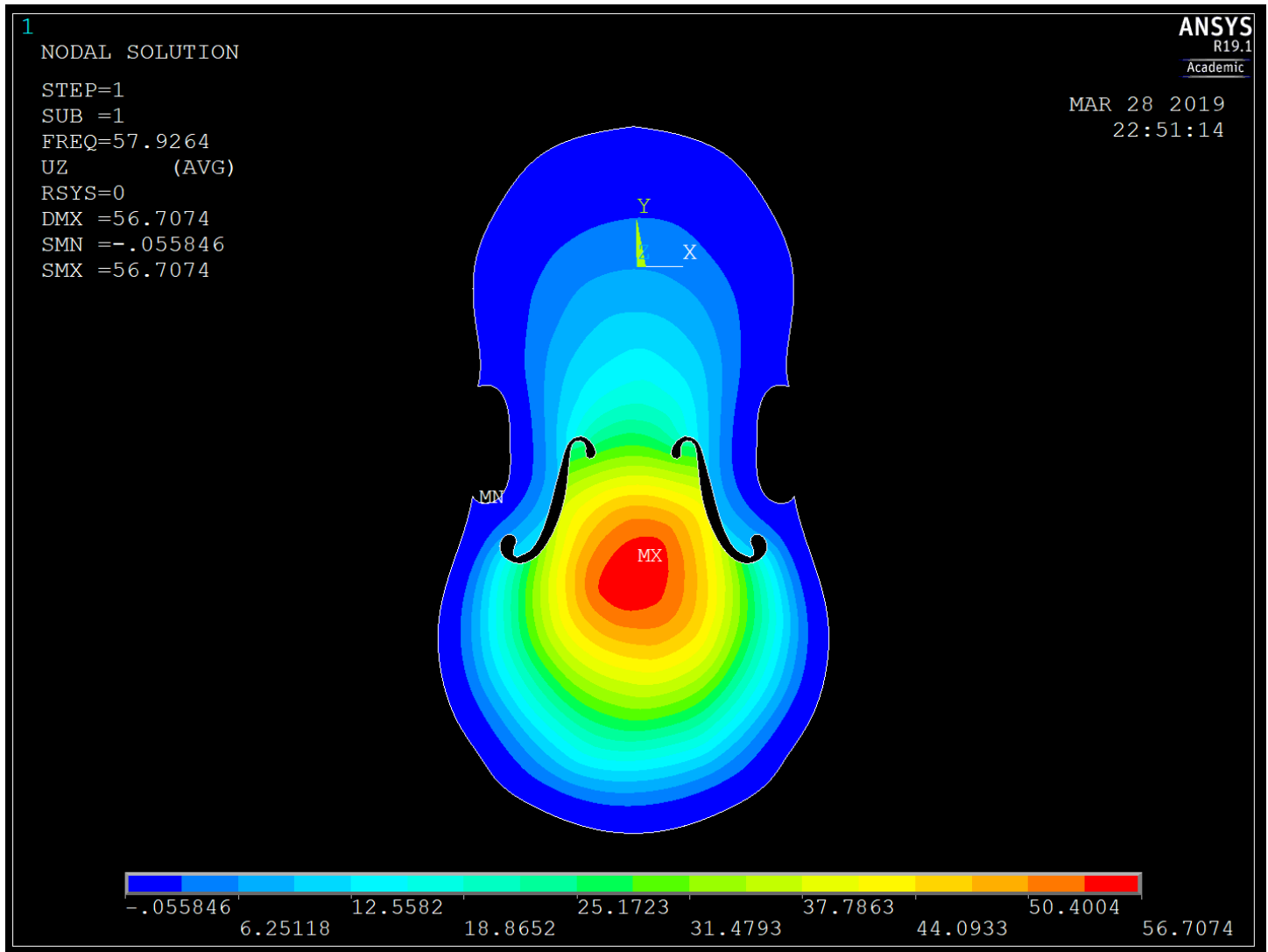


Figure 34: 5th Model Mode 1 Natural Frequency Z-Displacement Contour Plot

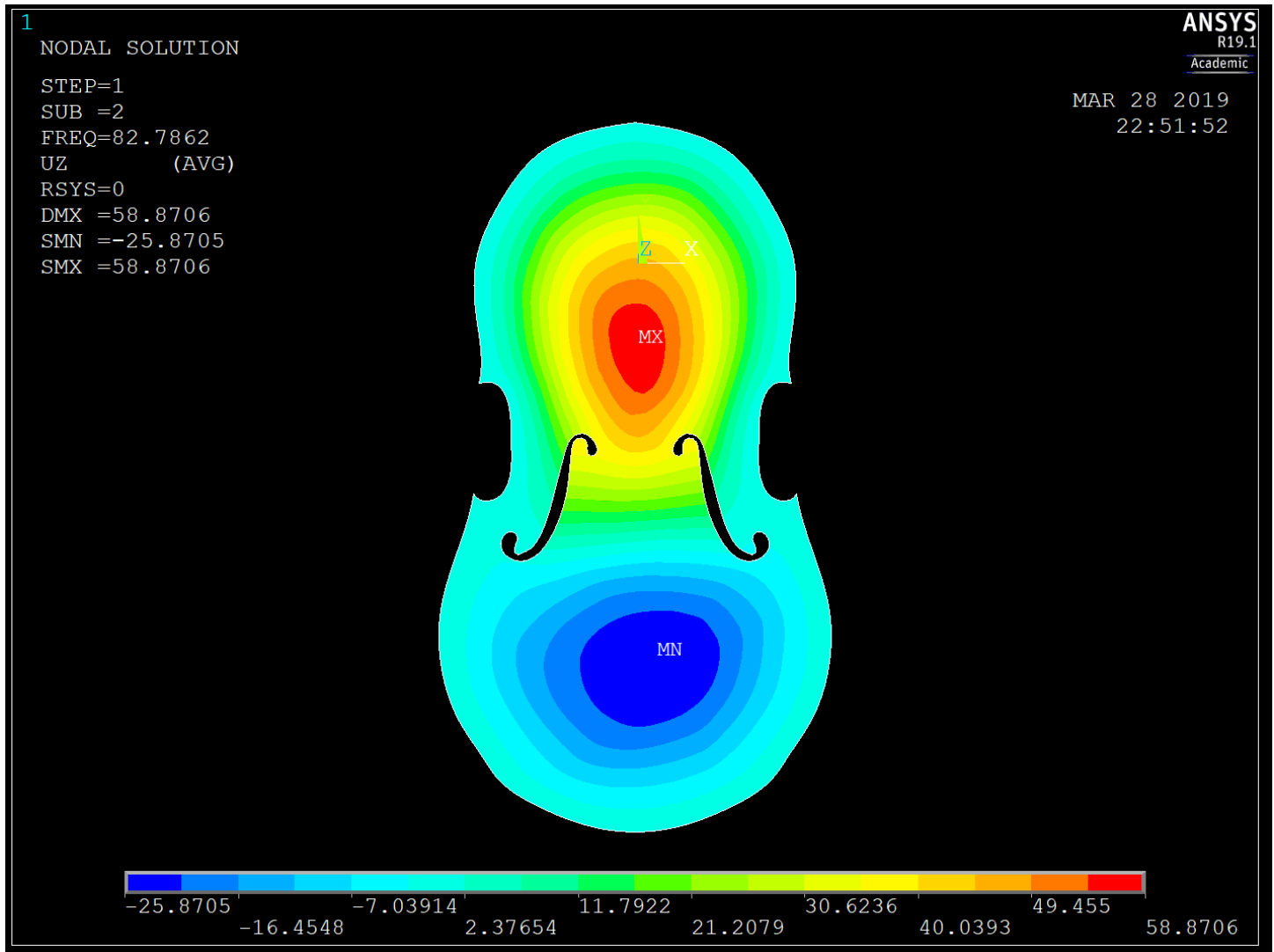


Figure 35: 5th Model Mode 2 Natural Frequency Z-Displacement Contour Plot

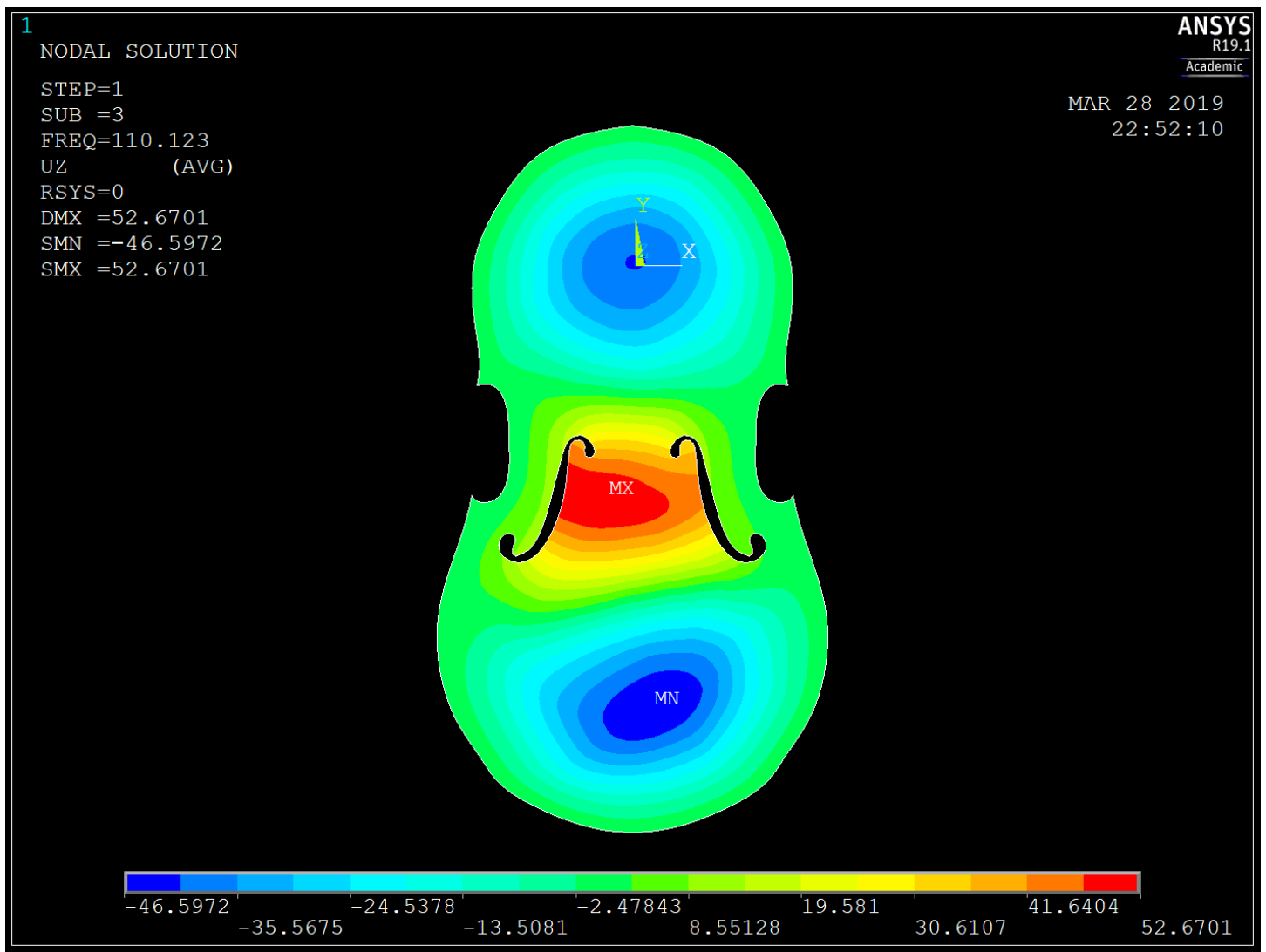


Figure 36: 5th Model Mode 3 Natural Frequency Z-Displacement Contour Plot



Figure 37: 5th Model Mode 4 Natural Frequency Z-Displacement Contour Plot

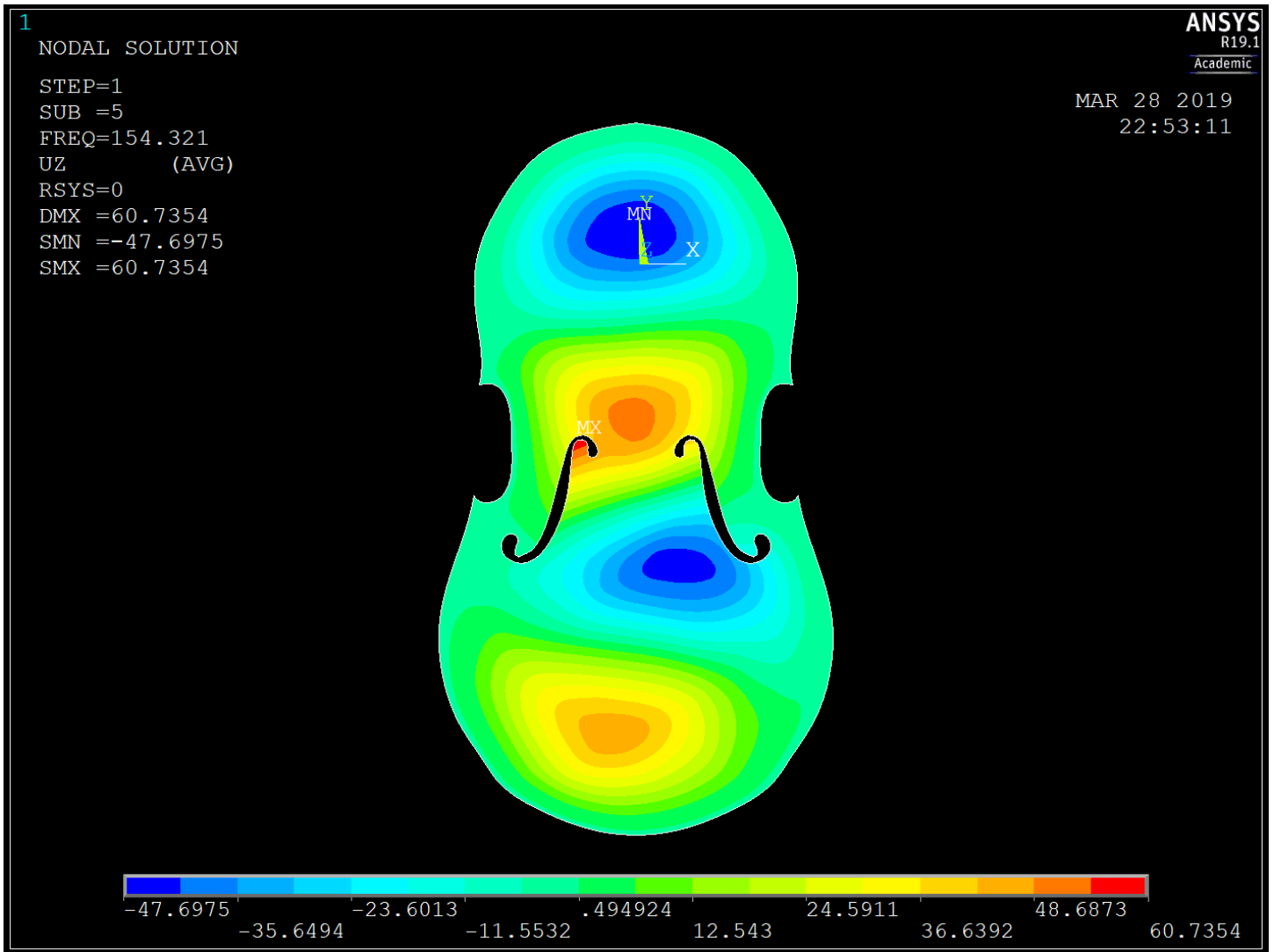


Figure 38: 5th Model Mode 5 Natural Frequency Z-Displacement Contour Plot

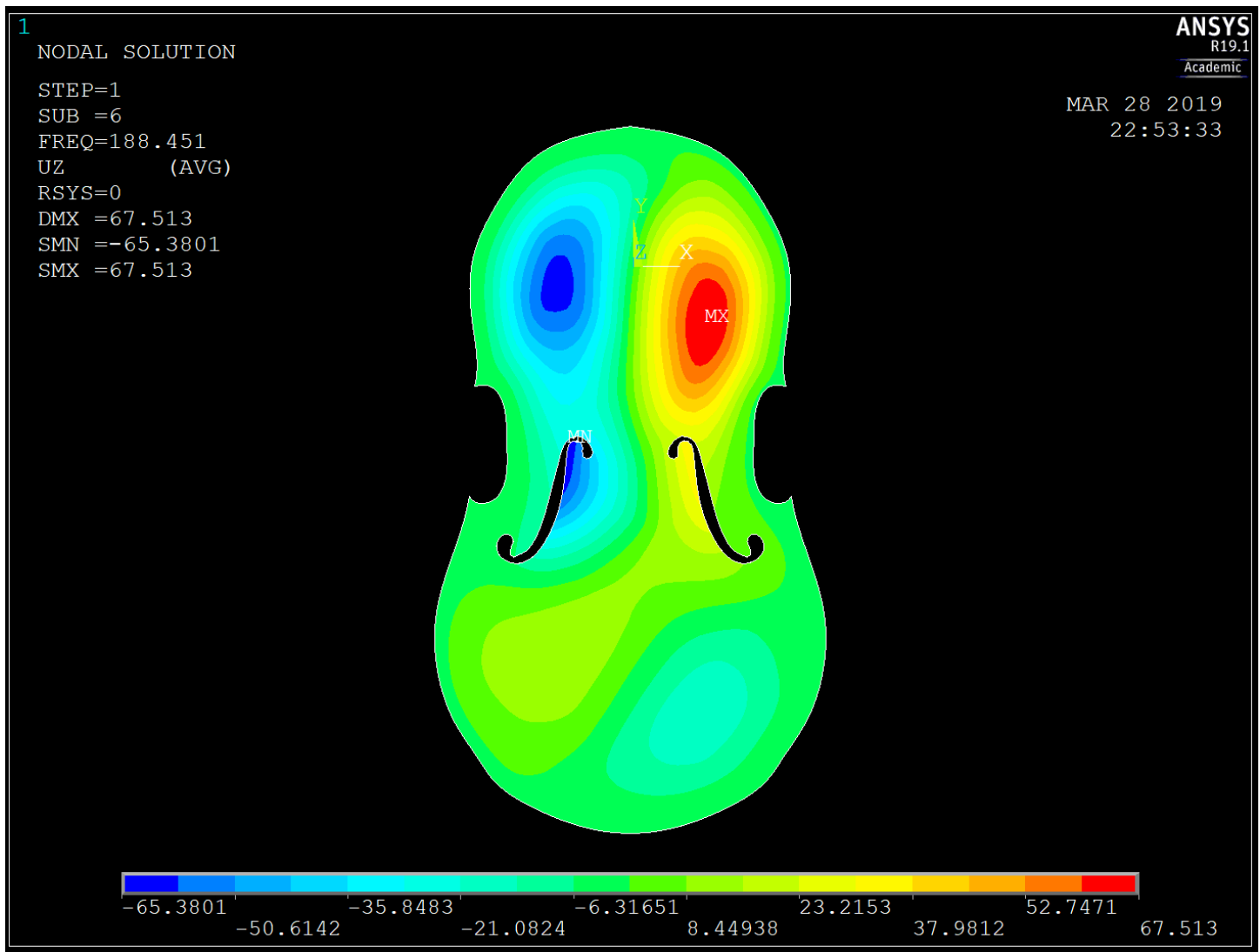


Figure 39: 5th Model Mode 6 Natural Frequency Z-Displacement Contour Plot

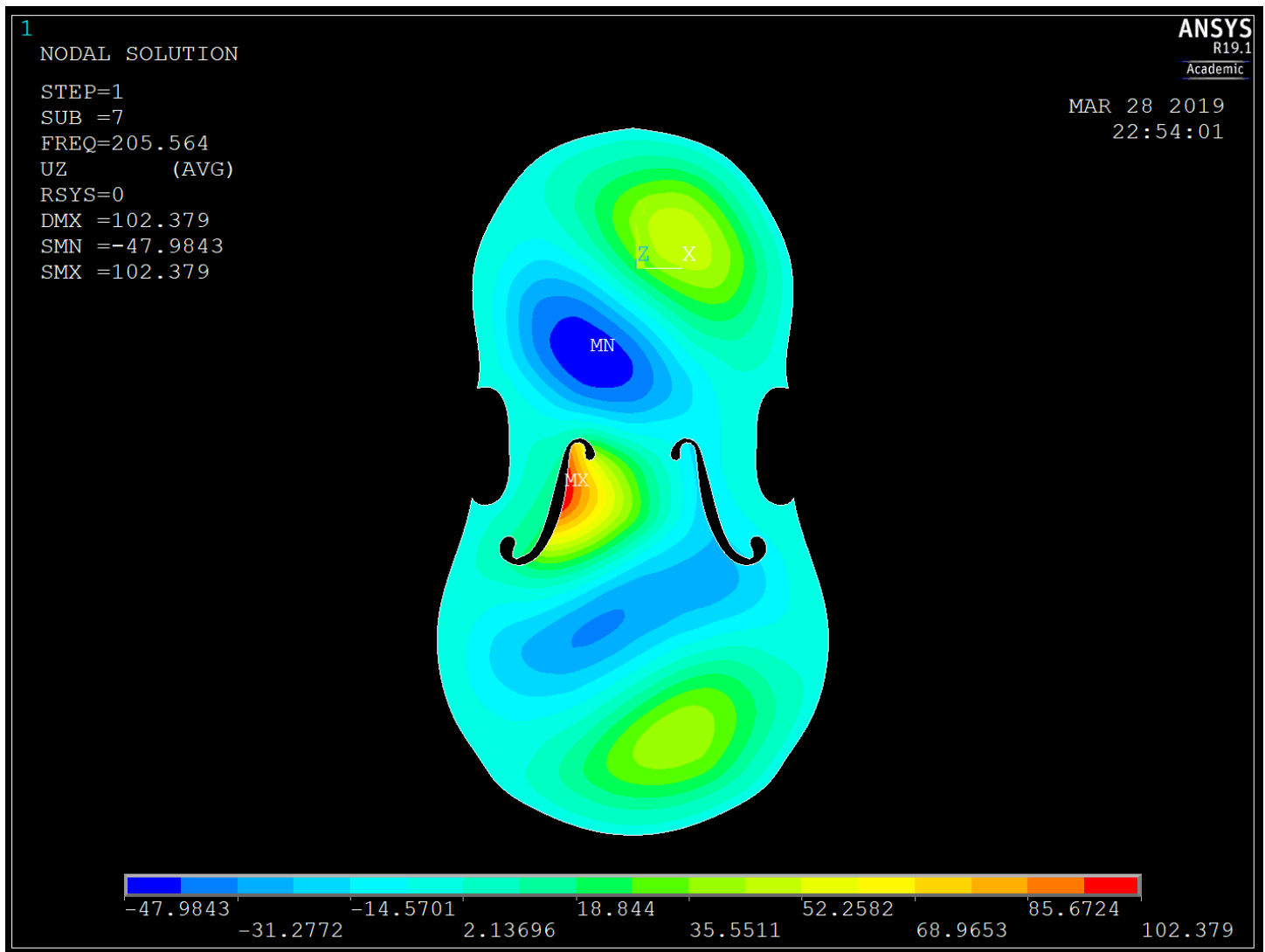


Figure 40: 5th Model Mode 7 Natural Frequency Z-Displacement Contour Plot

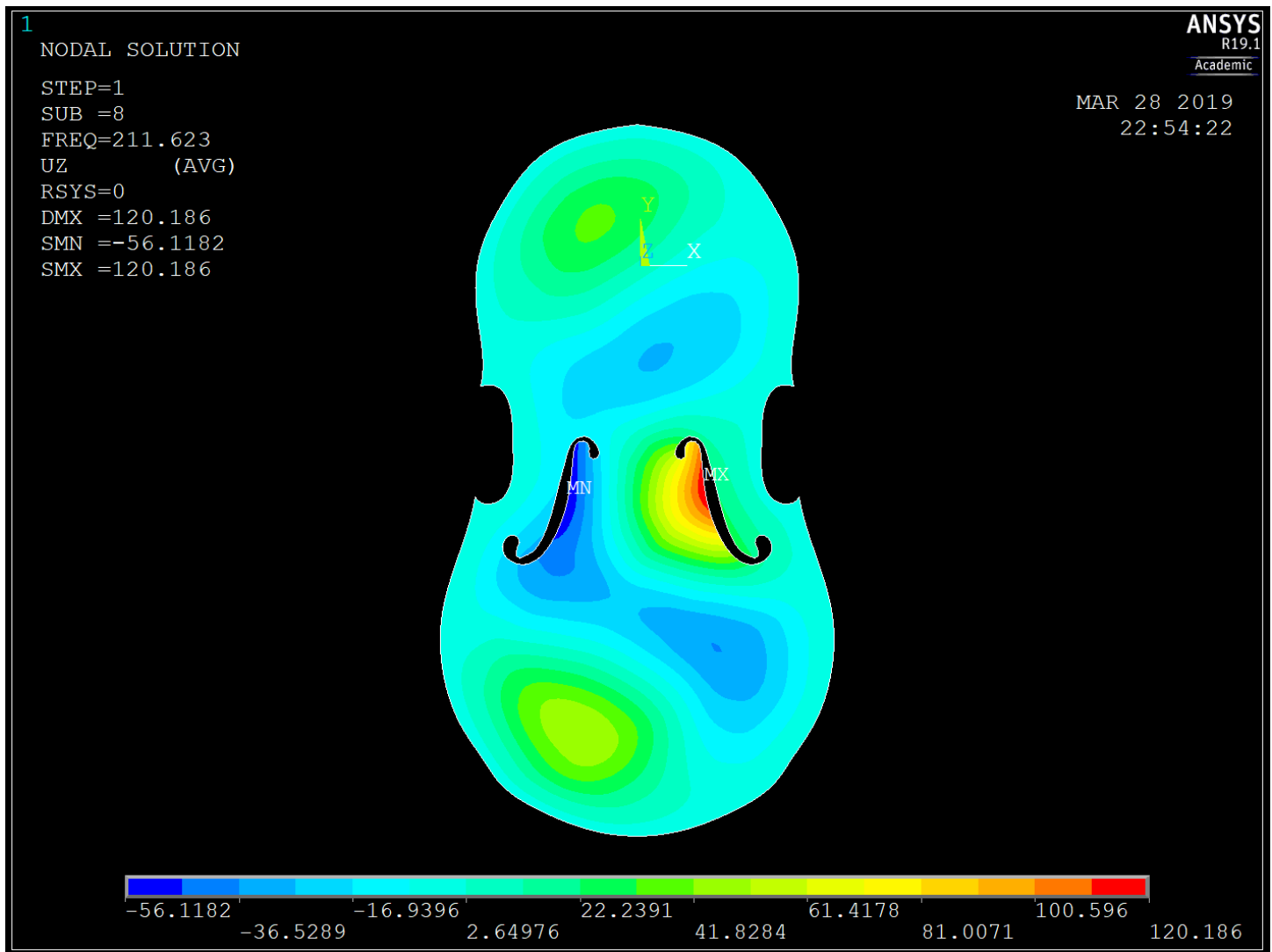


Figure 41: 5th Model Mode 8 Natural Frequency Z-Displacement Contour Plot

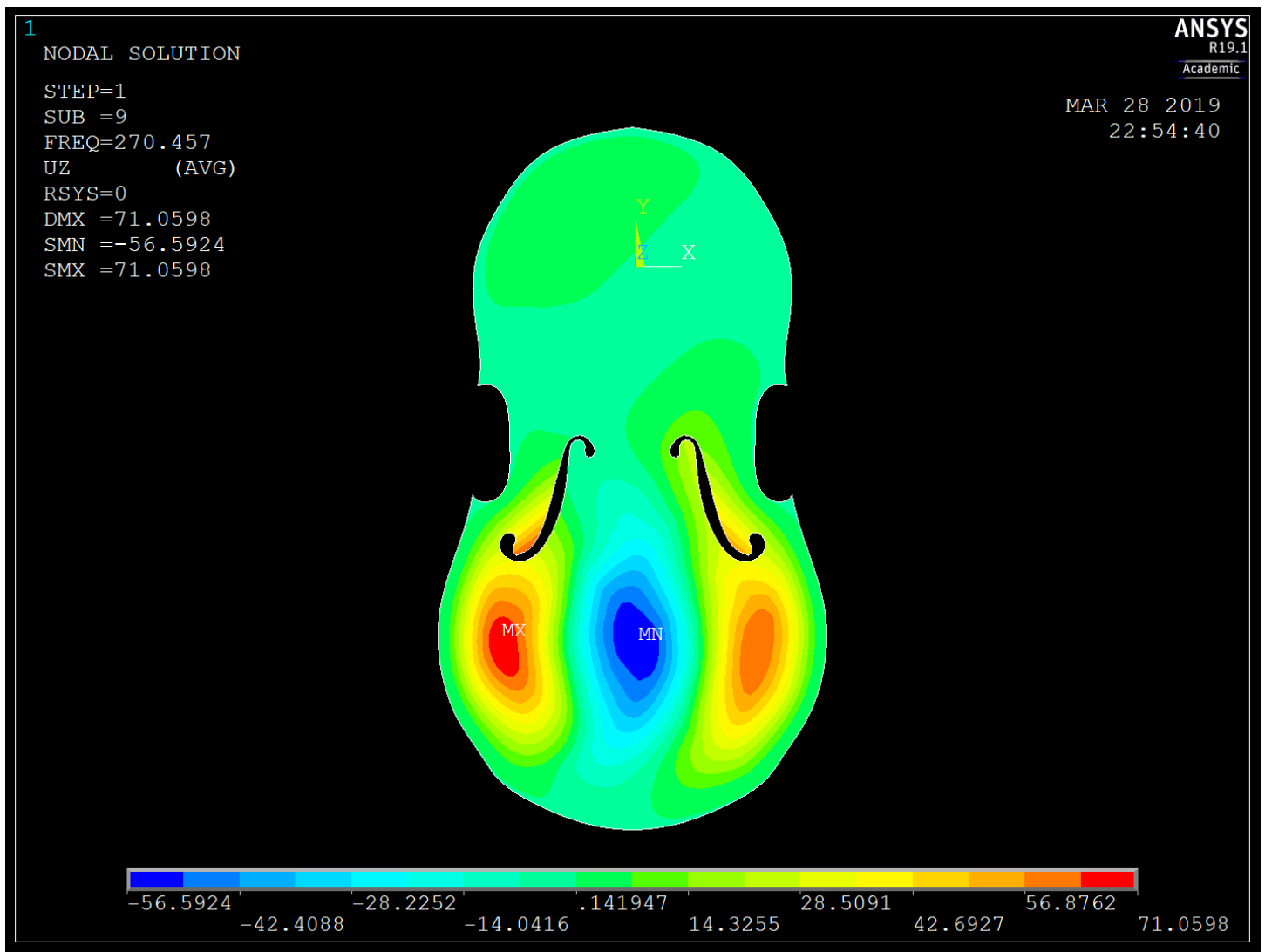


Figure 42: 5th Model Mode 9 Natural Frequency Z-Displacement Contour Plot

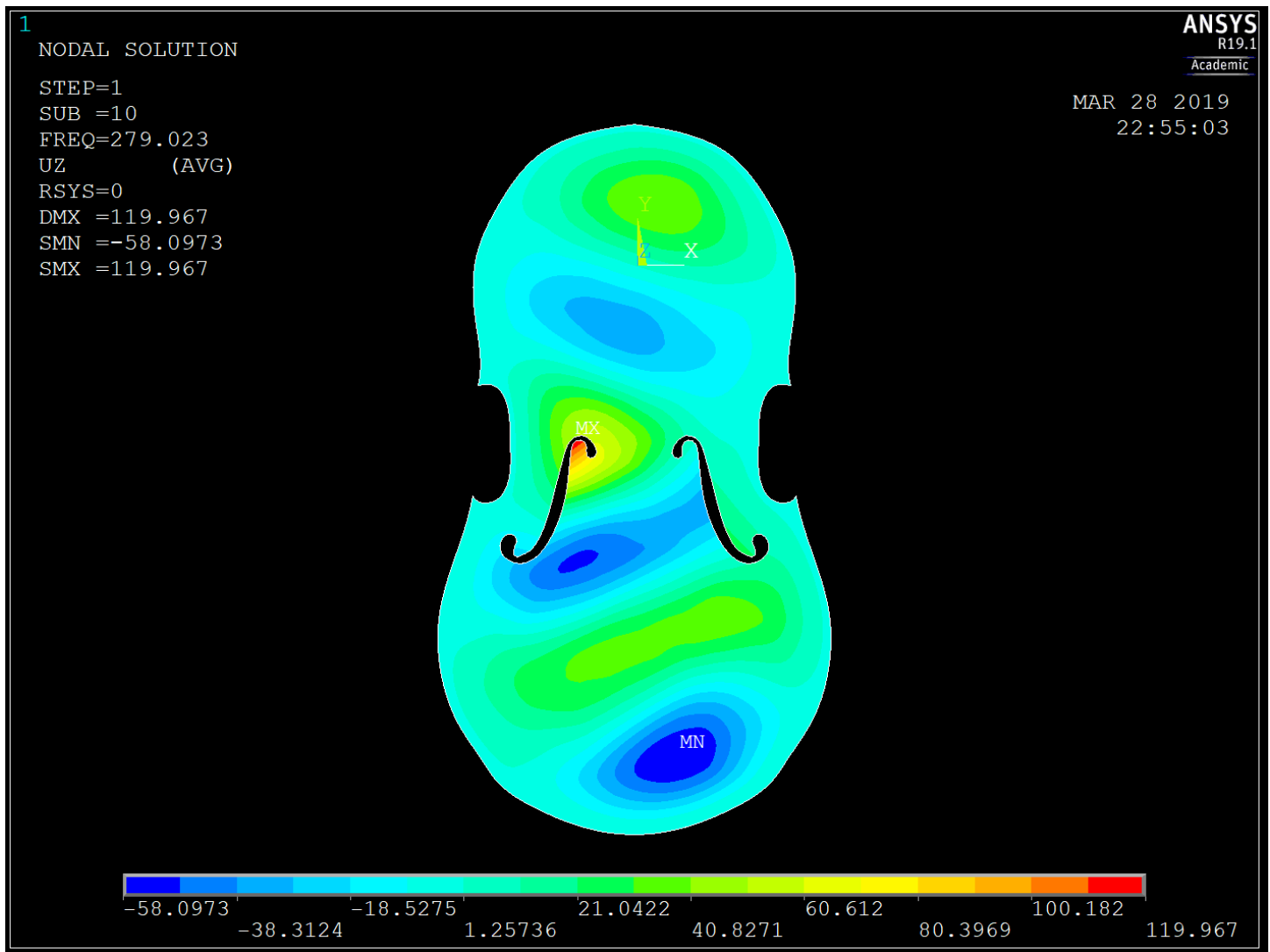


Figure 43: 5th Model Mode 10 Natural Frequency Z-Displacement Contour Plot

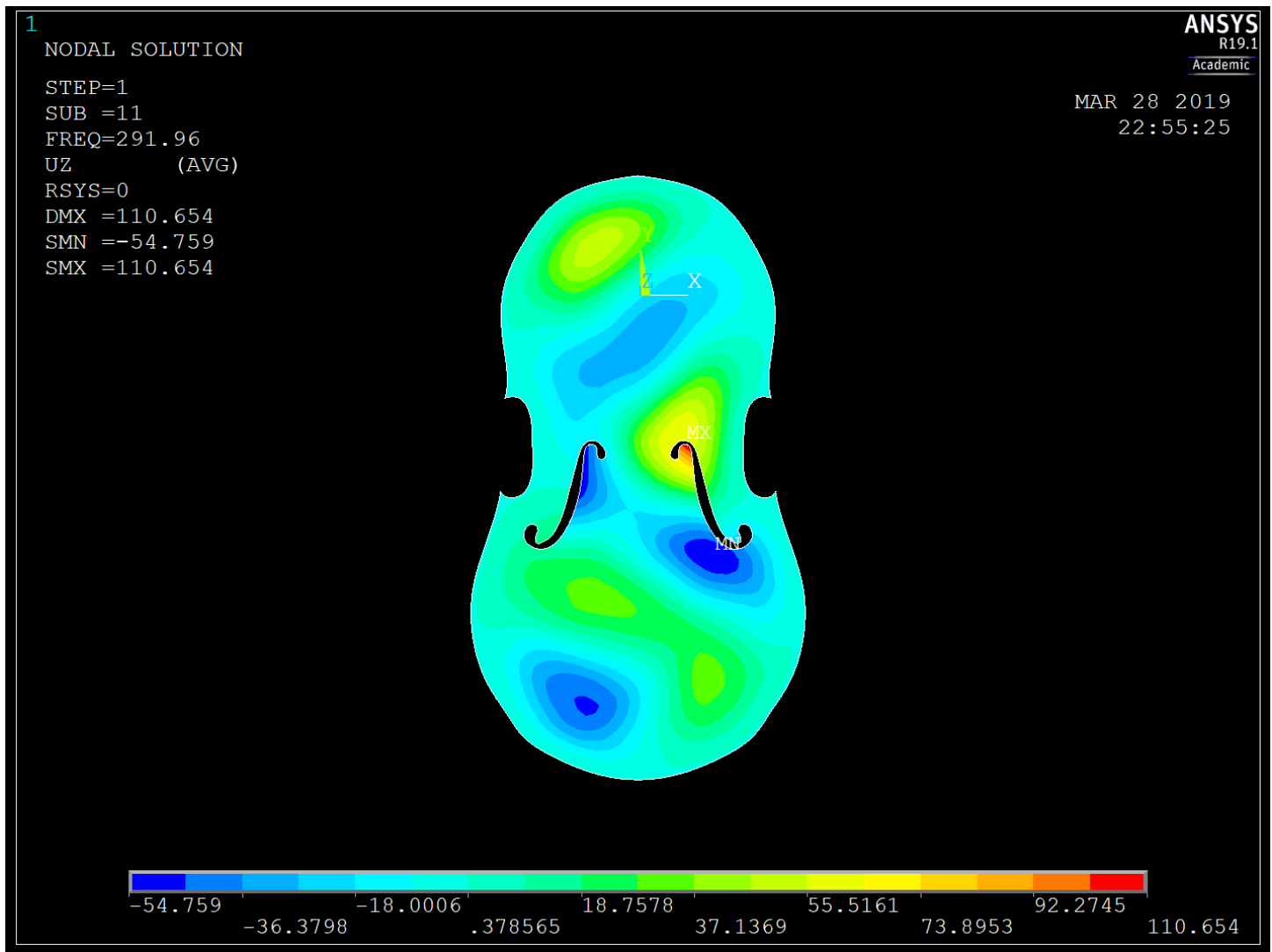


Figure 44: 5th Model Mode 11 Natural Frequency Z-Displacement Contour Plot

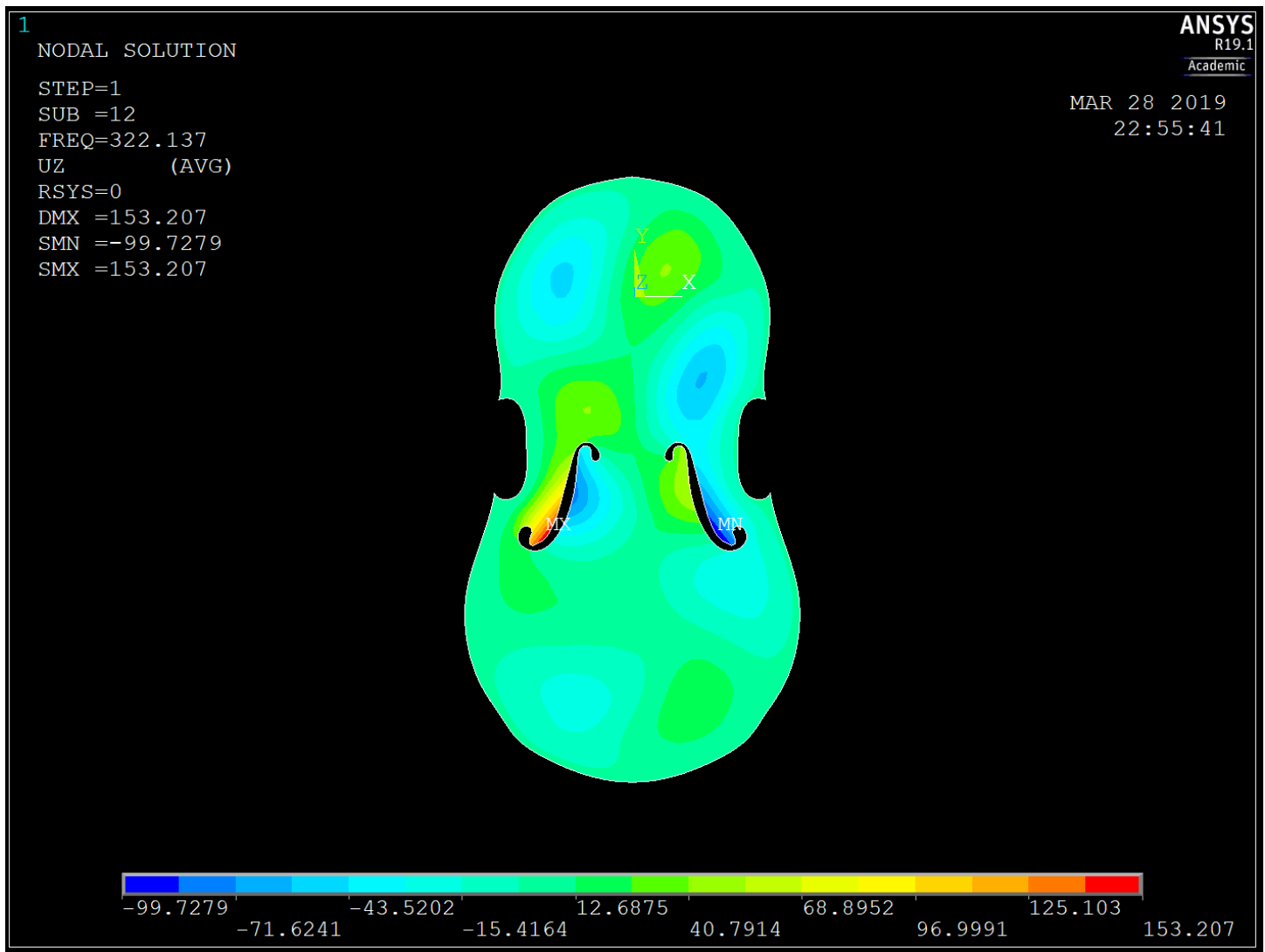


Figure 45: 5th Model Mode 12 Natural Frequency Z-Displacement Contour Plot